—Reviews—

ファージディスプレイ法を用いた腫瘍組織血管抗体の創製

山下琢矢,*,[a,b,c] 宇都口直樹,[a] 鈴木　亮,[a] 長野一也,[b]
角田慎一,[b,d] 堤　康央,[b,c,d] 丸山一雄[a]

Development of Anti-tumor Blood Vessel Antibodies by Phage Display Method

Takuya YAMASHITA,*,[a,b,c] Naoki UTOGUCHI,[a] Ryo SUZUKI,[a] Kazuya NAGANO,[b]
Shin-ichi TSUNODA,[b,d] Yasuo TSUTSUMI,[b,c,d] and Kazuo MARUYAMA[a]

[a]*Department of Biopharmaceutics, School of Pharmaceutical Sciences, Teikyo University, Suarashi1091-1, Sagamiko, Sagamihara, Kanagawa 229-0195, Japan,* [b]*Laboratory of Pharmaceutical Proteomics, National Institute of Biomedical Innovation, 7-6-8 Saito-Asagi, Ibaraki, Osaka 567-0085, Japan,* [c]*The Department of Toxicology, School of Pharmaceutical Sciences, Osaka University, 1-6 Yamadaoka, Suita, Osaka 565-0871, Japan, and* [d]*The Center for Advanced Medical Engineering and Informatics, Osaka University, 2-2 Yamadaoka, Suita, Osaka 565-0871, Japan*

(Received August 31, 2009)

Tumor blood vessels are essential for tumor growth. Therefore, these blood vessels are potential targets for anti-cancer therapy. The purpose of this study is to develop anti-tumor endothelial cell (TEC) antibodies for delivering anti-cancer agents or drugs. To achieve this goal, we utilized the phage antibody display library method to create monoclonal antibodies *in vitro*. Accordingly, we developed anti-TEC antibodies from an single chain Fv fragment (scFv) phage display library prepared using the Fv genes amplified from the mRNAs isolated from the TEC-immunized mice. The size of the phage antibody library prepared from the mRNA of the TEC-immunized mice was approximately 1.3×10^7 CFU. To select and enrich for the phages displaying the anti-TEC antibodies, cell panning was performed first using the TEC followed by subtractive panning using the normal endothelial cell. After five cycles of panning, the affinity of bound phage clones increased approximately 10 000 folds. Subsequently, clones isolated from the post-panning output library were tested for their antigen-specificity by ELISA and western blotting. One of the scFv phage clones showing antigen-specificity recognized only TEC *in vitro*, and when injected into the Colon26 bearing mice, this clone accumulated more on the tumor tissue than the wild type phage. These results suggest that the isolated an antibody and this clone's target molecule could be potentially useful for novel anti-tumor therapies.

Key words——tumor endothelial cell; phage display; antibody

1. はじめに

医療技術の進歩に伴い，各種疾患の治療成績は年々向上している一方で，「悪性新生物：がん」は1981年にわが国における死因の第1位となって以来，その死亡者は年々増加し，現在では死因全体の約3割を占めている．このように，「がん」を克服できていない現状から，新たながん治療法，診断法の確立が待望されている．

腫瘍組織は，その体積が1 mm³を超えて増大する際，血管より最も離れた中心部位は低酸素状態にある．[1-3] そして，HIF等を介してその低酸素シグナルは腫瘍細胞に伝わり，腫瘍細胞がVEGF，b-FGF等の血管新生誘導因子を産生し，新たな血管を既存の血管より誘導してくることが知られている．[4-7] この腫瘍により誘導された血管は，腫瘍細胞への酸素・栄養の供給，腫瘍細胞からの老廃物の除去という腫瘍にとってまさにライフラインとも言うべき機能をしており，腫瘍組織の維持，増大に必要不可欠である．[8,9] さらに，この腫瘍組織血管の誘導は腫瘍の増大だけでなく，腫瘍血行性転移の経路

[a]帝京大学薬学部生物薬剤学教室（〒229-0195 神奈川県相模原市相模湖町1091-1），[b]独立行政法人医薬基盤研究所基盤的研究部創薬プロテオミクスプロジェクト（〒567-0085 大阪府茨木市彩都あさぎ7-6-8），[c]大阪大学大学院薬学研究科毒性学分野（〒565-0871 大阪府吹田市山田丘1-6），[d]大阪大学臨床医工学融合研究教育センター（〒565-0871 大阪府吹田市山田丘2-2）
*e-mail: t-yamashita@nibio.go.jp

本総説は，日本薬学会第129年会シンポジウムGS6で発表したものを中心に記述したものである．

としても機能している．このように腫瘍組織血管は腫瘍組織にとって必要不可欠な存在であるため，腫瘍組織血管に対して傷害を誘導することは腫瘍組織に致死的なダメージを与えることになり，腫瘍の退縮及び，転移の抑制が期待できる．このような背景も相まって，現在，この腫瘍組織血管を標的とするような分子標的医薬品の開発が盛んに進められている．

近年，疾患関連分子に対する分子標的治療を可能とするモノクローナル抗体が脚光を浴びている．その優れた抗原特異性から，モノクローナル抗体は診断薬[10-14]として，さらには最近，抗体医薬として応用が非常に注目され，研究，臨床開発が盛んに行われており，現在，基礎研究段階のものを含めれば，約400以上もの抗体医薬品の研究開発が進められているとされている．[15-20] また，2007年の抗体医薬品の世界市場は約263億3800万ドル（約2兆3800億円）で，2013年には約490億5500万ドル（約4兆4300億円）まで拡大すると予想され，まさに熾烈な研究合戦が世界規模で展開中である．本邦においても，乳がんにおいて過剰発現が認められるerbB2を標的とするTrastuzumab（Herceptin®），[21-23] がんの血管新生をターゲットとした抗VEGF中和抗体であるBevacizumab（Avastin®）[24,25]を始め，徐々に抗体医薬品が承認・上市されつつある．

腫瘍組織血管は正常組織血管と異なった性質を有している[26,27]ため，その細胞膜表面若しくは，分泌タンパク質に特異的なタンパク質，いわゆるバイオマーカーが存在している可能性が考えられるが，腫瘍組織血管特異的なバイオマーカー，及びその抗体については世界的に認められる分子はいまだに発見されていないというのが現状である．腫瘍組織血管特異的ではないが，唯一の重要な指標となっているのは血管新生において非常に重要なシグナル系であるVEGFファミリーのVEGFR1（Flt-1），VEGFR2（Flk-1/KDR）の発現上昇のみである．[28-30] そこで本研究では，新規がん治療薬，腫瘍組織血管特異バイオマーカー探索の強力なツールとなり得る，腫瘍組織血管特異タンパク質に対する抗体の創製を従来のハイブリドーマ法と比較して画期的な抗体創製法であるファージディスプレイ法を用いて試みた．

2. ファージディスプレイ法

ファージディスプレイ法は1985年にSmithらによって報告され，[31] バクテリオファージ内に存在するファージミドベクターへ外来遺伝子（ペプチド・タンパク質・抗体等）を導入することで，バクテリオファージ表面に目的分子を発現させることを可能とする技術であり，その分子はバクテリオファージのコートタンパク質（g3p）と融合した形態で発現している．抗体作製への応用は1990年にMcaffertyらが抗体機能ドメインを提示したファージディスプレイ法をハイブリドーマ法に代わる新しいモノクローナル抗体作製技術として報告したことに始まる．[32] 1991年にはMarksらが免疫していないヒトの末梢血リンパ球を出発材料に構築したファージ抗体ライブラリから，ヒト生体成分や，ターキー卵白アルブミン，ウシ血清アルブミンなど異種動物の抗原に対するファージ抗体の分離を報告した．[33]

繊維状ファージM13は環状の一本鎖ゲノムDNAを持ち，そのまわりに5つのコートタンパク質（g3p, g6p, g7p, g8p, g9p）が連結した細長い筒状の構造をしており，大腸菌に感染して増殖するウイルスである．ファージディスプレイは，これらのファージコートタンパクと外来ポリペプチドを融合した形で発現させることでファージ表面にディスプレイさせる方法である．

ファージディスプレイ法の特徴は，① 任意の外来分子をファージ表面に提示できること，② 1個の宿主菌に1個のファージしか感染しないため（pDNA incompatibilityに寄与する），各ファージ内の外来遺伝子とファージ表面に提示された外来遺伝子産物が一致していること，③ 種々の外来遺伝子産物を提示したファージを数億種類以上の多様性を有するライブラリとして容易に，かつ短期間（1週間以内）で調製できること，④ 宿主菌に感染させることで簡便に特定のファージを増幅できることにある．[34,35]

外来遺伝子として一本鎖抗体（single chain variable fragment: scFv）遺伝子を用いるファージ抗体ライブラリは，ファージ表面に数十万から数億以上のレパートリーを有する抗体機能性ドメインであるVL領域とVH領域をリンカーで連結したscFv抗体を発現させるものである（Fig. 1）．このライブラリから標的タンパク質へ特異的に結合するクローンを選択・回収し，増幅する操作（パンニング）を繰り返すことによって，標的タンパク質に結合する

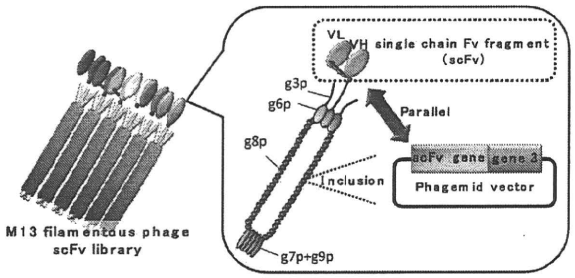

Fig. 1. The scFv Phage Display System

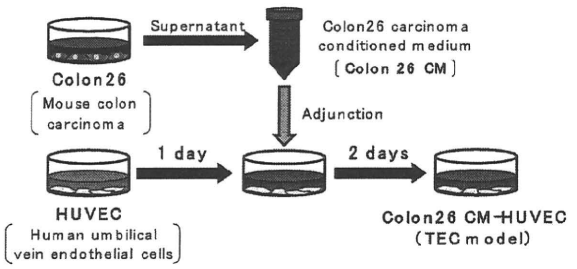

Fig. 2. Development of the Tumor Endothelial Cell Model
Human umbilical vein endothelial cells (HUVEC) cultured in Colon26 carcinoma-conditioned medium (Colon26 CM-HUVEC) were used as model TECs.

scFv 抗体分子を表面提示したファージをスクリーニングすることが可能である.[36,37] しかも得られたファージは目的抗体をコードする遺伝子を内封しているため，抗体の遺伝子配列も同時に獲得することが可能である．このように，ファージディスプレイ抗体ライブラリは *in vitro* で生体内の抗体産生系を模倣し，さらに生体の免疫系から独立した抗原の種類を選ばない優れた抗体創製システムとして，抗体医薬開発に大きく貢献している．

3. 抗腫瘍組織血管抗体の創製

3-1. 腫瘍組織血管内皮細胞モデル　抗腫瘍組織血管抗体を創製するためには，腫瘍組織血管内皮細胞を獲得しなければならないが，腫瘍組織血管内皮細胞のみを生体内腫瘍組織から単離することは非常に困難である．そこで筆者らはがん細胞の培養上清（Conditioned Medium: CM）を用いることで，*in vivo* の腫瘍組織血管内皮細胞を模倣した腫瘍組織血管内皮細胞モデルを *in vitro* の系で再構築し，このモデル細胞から抗原タンパク質を調製後，これを用いて抗体創製を試みた．本検討ではマウス結腸がん細胞（Colon26）の CM で培養したヒト臍帯静脈血管内皮細胞（HUVEC）を腫瘍組織血管内皮細胞モデル（Colon26 CM-HUVEC）とした（Fig. 2）．

この腫瘍組織血管内皮細胞モデルは，生体内腫瘍組織血管内皮細胞に特徴的な性質である細胞間透過性の亢進を示し,[38] また腫瘍組織血管内皮細胞モデルの膜抗原を樹状細胞にパルス後，この樹状細胞をマウスに免疫したところ，*in vivo* において，副作用を引き起こすことなく腫瘍組織血管特異的な傷害性が誘導され，それに伴う抗腫瘍効果が観察された（未発表データ）．さらには，2 次元電気泳動解析により，その特異的抗原タンパク質の存在が明らかとなった（未発表データ）．

これらのことから，この腫瘍組織血管内皮細胞モデルは生体内の腫瘍組織血管内皮細胞と全く同じ特異的抗原タンパク質を発現している可能性が非常に高いと考えられる．

3-2. 腫瘍組織血管内皮細胞モデル免疫抗体ライブラリの作製　現在，ファージ抗体ライブラリとしては，免疫していない動物や健常人の B 細胞を由来とした「ナイーブファージ抗体ライブラリ」[39,40] と免疫した動物や疾患患者の B 細胞を由来とした「免疫ファージ抗体ライブラリ」[41] の 2 種類が主に用いられている．各ライブラリにはそれぞれ長所・短所があり，「ナイーブファージ抗体ライブラリ」は抗体遺伝子に偏りのない多様性に富んだ抗体ライブラリを獲得できるという長所を持つ一方で，抗原結合力の強い抗体を得ることが困難であるという短所も持ち合わせている．また,「免疫ファージ抗体ライブラリ」は抗原結合力の強い抗体を得ることができるという長所を持つ一方で，免疫状態に偏りがあるため，「ナイーブファージ抗体ライブラリ」と比較して得られる抗体ライブラリは多様性に乏しいという短所を持つ．このように両ライブラリは一長一短であるため，目的に合わせて使い分ける必要がある．

本検討では最終的に獲得した抗体を抗原探索・解析のツールとしてだけでなく，ドラッグデリバリーのツールとして用いる狙いがあるため，より強力な結合力を有する抗体を獲得可能な「免疫ファージ抗体ライブラリ」を作製した．

免疫原として腫瘍血管内皮細胞モデルである Colon 26 CM-HUVEC を BALB/c マウスに一週間おきに 2 回免疫を行った．次に，マウスの Colon26 CM-HUVEC に対する抗体価を測定後，脾臓を回収

し，mRNA を回収した．続いて，この mRNA をテンプレートに cDNA を作製し，PCR により抗体の VL, VH 領域の DNA の増幅を行った．さらに，増幅した VL, VH 領域の DNA を連結させる assembly PCR を行い，scFv DNA を作製した．そして，この scFv DNA をファージミドベクター（pCANTAB5E）へクローニングした．最後にクローニング後のファージミドベクターを大腸菌（TG1）へエレクトロポレーションにより導入した．構築したライブラリのライブラリサイズは大腸菌の形質転換効率より算出した．その結果，構築した抗体ライブラリは 1.3×10^7 CFU という抗体多様性を保持していた（Fig. 3）．

3-3. 抗腫瘍組織血管抗体のスクリーニング

機能性分子を獲得するためのスクリーニング系の設計はファージディスプレイ法のみならず，ディスプレイ技術を駆使する場合のキーテクノロジーとして重要視される．精製抗原が入手可能な場合は，固層化法（パンニング）やビオチン化抗原とストレプトアビジン固定化担体を用いたスクリーニング方法が主要な選択系として用いられている．しかし，各スクリーニングを効率よく行うためには，対照抗原の目的エピトープを被覆，あるいは変性させない工夫が必要であり，さらには反応温度や洗浄条件，塩濃度など複数の要因が影響する．

今回，われわれは精製された抗原タンパク質を獲得しているため，抗体ライブラリから抗腫瘍組織血管抗体を選別するスクリーニング系として簡便なパンニングを選択した．パンニングはファージ抗体ライブラリ内から，固層化した標的タンパク質へ特異的に結合するクローンを選択・回収し，増幅する操作であり，このパンニングを繰り返すことによって，標的タンパク質に結合する scFv 抗体分子を表面提示したファージを選別・濃縮することが可能である（Fig. 4）．

近年，臨床で用いられている抗体医薬品は細胞膜表面の膜タンパク質，若しくは血中に遊離している機能性タンパク質（レセプターアゴニスト等）を認識する抗体である．今回創製する抗体の将来的な展望として，創出した抗体をドラッグデリバリー，また診断のツールとして使用することを目的としているため，創製する抗体は細胞内タンパク質ではなく，細胞外表面上の膜タンパク質を認識する抗体であることが必須条件であると考えられる．このことから，われわれはパンニングにより抗体を選別する際に用いる標的抗原には，調製時に破壊された細胞の細胞内タンパク質が混入する恐れのある，細胞抽出抗原タンパク質（細胞ライセート，ブタノール抽出膜抗原タンパク質等）を用いるのではなく，生細胞をそのまま標的抗原として用いることが最適であると考えた．

さらに，抗腫瘍組織血管抗体を創製するにあたって，われわれが非常に重要であると考えていることは，いかに副作用の少ない抗体を選別するかである．腫瘍組織血管は正常組織血管内皮細胞が腫瘍細胞の産出する液性因子（サイトカイン，ケモカイ

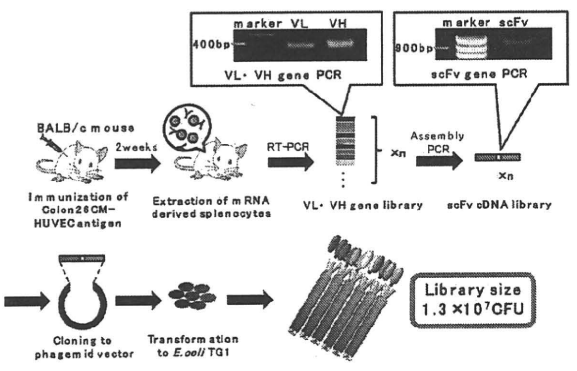

Fig. 3. Development of the Tumor Endothelial Cell Immune Antibody Library

The single chain antibody fragment variable (scFv) phage display library was prepared by amplifying the Fv genes from the mRNA derived from the TEC-immunized murine splenocytes.

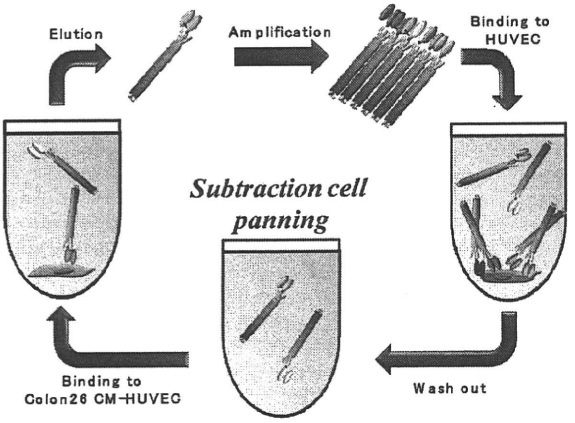

Fig. 4. Antibody Selection by Subtraction Cell Panning

Anti-TEC antibodies were selected by cell panning against Colon26 CM-HUVEC with subtractive panning against normal HUVEC.

ン，増殖因子等）により腫瘍組織へ誘導され，増殖することで，形成されると考えられている．このため，腫瘍組織血管内皮細胞は正常組織血管内皮細胞と構成タンパク質の大部分が類似していると考えられる．事実，われわれが構築した腫瘍組織血管内皮細胞モデルにおいても，2D-DIGE 比較解析の結果，正常組織血管内皮細胞と構成タンパク質の大部分が類似していた．このことからも，パンニングの際，腫瘍組織血管内皮細胞モデルのみを用いてしまうと，正常組織血管内皮細胞と交差性を持つ抗体が選別されてくる可能性が非常に高い．そこで，腫瘍組織血管内皮細胞モデルと抗体ライブラリファージを結合させる前に，正常組織血管内皮細胞と結合させるサブトラクションセルパンニングを行うことで腫瘍組織血管内皮細胞モデル特異抗体の選別・濃縮を図った（Fig. 4）．

まず，抗体ライブラリファージを HUVEC と結合させ，正常組織血管と結合する抗体ファージを除去し，遊離している抗体ファージを Colon26 CM-HUVEC と結合させた．非特異的結合ファージを洗浄後，Colon26 CM-HUVEC 結合抗体ファージを回収し，大腸菌に感染させ，増幅した．このサブトラクションパンニングを計 5 回行った結果，パンニング前のファージ抗体ライブラリ（input ファージ）とパンニングにより回収されたファージ（output ファージ）の比率は，5th パンニング時では，1st パンニング時と比較して，約 10000 倍という高い比率を示したことから，Colon26 CM-HUVEC 特異的に結合する抗体ファージの選別・濃縮に成功したと推測される（Fig. 5）．

さらに，抗体アミノ酸配列を確認するため，各パンニングラウンドのファージ抗体をモノクローン化後，インサート PCR を行い，scFv DNA の増幅が確認されたクローンの scFv アミノ酸シークエンスを解析した．その結果，2 種類の scFv のアミノ酸シークエンス解析に成功した（未発表データ）．獲得した 2 種類の scFv は抗体の抗原認識性を決定する上で非常に重要である 3 ヵ所の相補性決定領域（complementarity-determining regions: CDR1, CDR2, CDR3）を保有し，最も多様性に富むとされている CDR3 領域の中で特に，VH の CDR3 領域においては，アミノ酸の種類，数ともに全く異なっていた．

3-4. 獲得抗体の特性評価　獲得抗体の *in vitro* における抗体特性評価として，ELISA, western blotting による抗原結合性評価，及び抗原分子量の探索を行った（Fig. 6）．

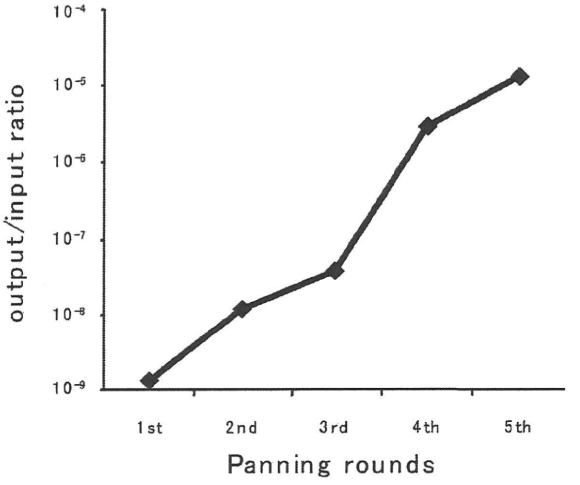

Fig. 5. Enrichment of Antibodies to Tumor Endothelial Cell Model by Subtraction Cell Panning

ELISA による抗原結合性評価の結果，Clone 1 ファージ抗体は，Colon26 へは結合性は示さない一方で，Colon26 CM-HUVEC へは HUVEC への結合性と比較して約 2 倍の抗原結合性を示した．さらにこのファージ抗体の抗原分子量を探索するため，Clone 1 ファージ抗体を用いて western blotting を行った．

Western blotting の結果，Clone 1 ファージ抗体は分子量約 45000 Da のタンパク質に対して結合性を示し，そのバンドの発光強度は ELISA での結果とほぼ相関していた．また，この抗原タンパク質は腫瘍組織血管に高発現しているとされている VEGFR2 とは異なる分子量を示していたことから，VEGFR2 以外の新規腫瘍組織血管マーカーである可能性がある．

さらに獲得抗体の *in vivo* での腫瘍組織集積性を評価するため，獲得ファージ抗体を担がんマウスへ静注し，全身灌流後，腫瘍組織を摘出した．その腫瘍組織内のファージ titer を計測することで獲得抗体の腫瘍組織集積能を評価した．*In vitro* における Colon26 CM-HUVEC への抗原結合性を示した Clone 1 ファージ抗体を担がんマウスへ投与したところ，有意差は得られなかった（$p = 0.08$）が Clone 1 ファージ抗体は野生型ファージと比べて約

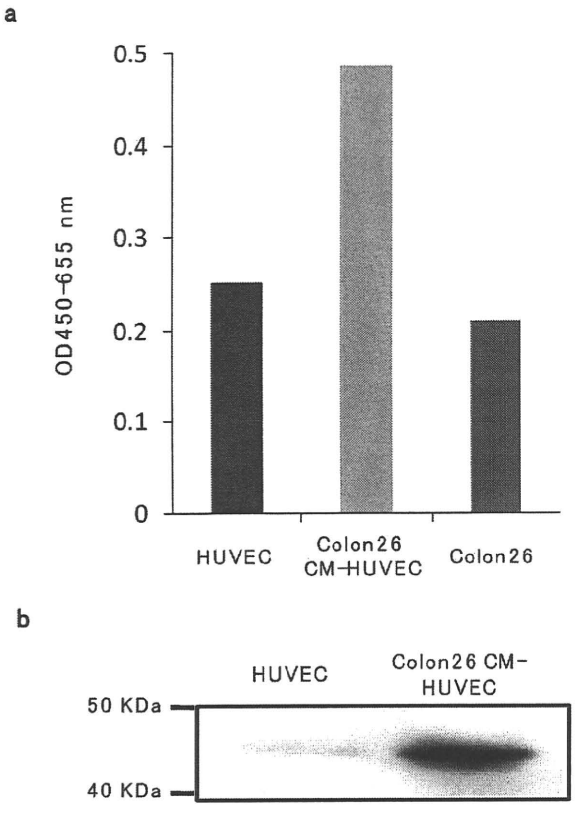

Fig. 6. Evaluation of Antibody Binding Activity *in Vitro*
(a: ELISA, b: Western blot). The binding specificities of the phage antibodies were assessed *in vitro* by using ELISA and Western blotting.

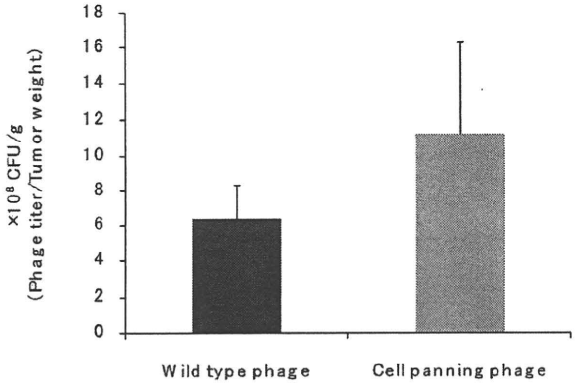

Fig. 7. Evaluation of Antibody Binding Activity in a Pilot Study *in Vivo*
The binding specificities of the phage antibodies were assessed *in vivo* by analyzing their accumulation on the tumor tissue. $n=3$, $p=0.08$.

1.8倍の腫瘍集積性を示す傾向にあった（Fig. 7）．この有意差が得られなかった原因は，抗体をファージ上に提示した状態で用いていることから，ファージが持つ非特異的吸着性の影響を受け，本来得られるべき差異がマスクされてしまったためとわれわれは推測している．そこで今後，より詳細に獲得した抗体の抗原認識性を評価するため，得られたClone 1の遺伝子をもとに，抗体のみを精製し，再検討する予定である．なお，Clone 2に関しても現在，同様に特性評価を行っている．

4. おわりに

本研究の結果，抗腫瘍組織血管抗体の創製に成功した．今後は免疫沈降法，質量分析法を駆使して各抗体の抗原タンパク質を同定し，それら抗原タンパク質の機能，生体分布評価を行う予定である．将来的に本研究により創製した抗体，その抗原が，がん治療，診断及び腫瘍組織血管研究の進展に大きく貢献することを期待している．

REFERENCES

1) Semenza G. L., *J. Clin. Invest.*, **106**, 809–812 (2000).
2) Yu J. L., Rak J. W., Coomber B. L., Hicklin D. J., Kerbel R. S., *Science*, **295**, 1526–1528 (2002).
3) Blagosklonny M. V., *Cancer Cell*, **5**, 13–17 (2004).
4) Klagsbrun M., Sasse J., Sullivan R., Smith J. A., *Proc. Natl. Acad. Sci. USA*, **83**, 2448–2452 (1986).
5) Montesano R., Vassalli J. D., Baird A., Guillemin R., Orci L., *Proc. Natl. Acad. Sci. USA*, **83**, 7297–7301 (1986).
6) Frater-Shroder M., Risau W., Hallmann R., Gautschi P., *Proc. Natl. Acad. Sci. USA*, **84**, 5277–5281 (1987).
7) Carmeliet P., *Nat. Med.*, **6**, 389–395 (2000).
8) Folkman J., *J. Natl. Cancer Inst.*, **82**, 4–6 (1990).
9) Keller R., Pratt B. M., Furthmary H., Madri J. A., *Am. J. Pathol.*, **128**, 299–306 (1987).
10) Aburatani H., *J. Gastroenterol.*, **40** (Suppl. 16), 1–6 (2005).
11) Mume E., Orlova A., Malmström P.-U., Lundqvist H., Sjöberg S., Tolmachev V., *Nucl. Med. Biol.*, **32**, 613–622 (2005).
12) Peknicova J., Chladek D., Hozak P., *Am. J. Reprod. Immunol.*, **53**, 42–49 (2005).
13) Andresen H., Grötzinger C., Zarse K., Kreuzer O. J., Ehrentreich-Förster E., Bier F. F.,

Proteomics, **6**, 1376–1384 (2006).
14) Miyata T., Jige M., Nakaminami T., Uragami T., *Proc. Natl. Acad. Sci. USA*, **103**, 1190–1193 (2006).
15) O'Mahony D., Bishop M. R., *Front. Biosci.*, **11**, 1620–1635 (2006).
16) Schulze-Koops H., Lipsky P. E., *Curr. Dir. Autoimmun.*, **2**, 24–49 (2000).
17) Bhattacharya-Chatterjee M., Chatterjee S. K., Foon K. A., *Expert. Opin. Biol. Ther.*, **2**, 869–881 (2002).
18) Takeshita A., *Rinsho Byori*, **52**, 917–923 (2004).
19) González E., Gutiérrez E., Hernández Y., Roselló G., Gutiérrez M. J., Gutiórrez Martínez E., Manzanera M. J., García J. A., Praga M., Morales J. M., Andrés A., *Transplant. Proc.*, **37**, 3736–3737 (2005).
20) Cheson B. D., *Cancer Immunol. Immunother.*, **55**, 188–196 (2006).
21) Bohme C., *Eur. J. Oncol. Nurs.*, **4**, 30–36 (2000).
22) Carter P., Fendly B. M., Lewis G. D., Sliwkowski M. X., *Breast Dis.*, **11**, 103–111 (2000).
23) Murray S., *CMAJ*, **174**, 36–37 (2006).
24) Kim K. J., Li B., Winter J., Armanini M., Gillett N., Phillips H. S., Ferrara N., *Nature*, **362**, 841–844 (1993).
25) Presta L. G., Chen H., O'Connor S. J., Chisholm V., Meng Y. G., Krummen L., Winkler M., Ferrara N., *Cancer Res.*, **57**, 4593–4599 (1997).
26) Wu N., Klitzman B., Dodge R., Dewhirst M. W., *Cancer Res.*, **52**, 4265–4268 (1992).
27) Matsumura Y., Maeda H., *Cancer Res.*, **46**, 6387–6392 (1986).
28) Risau W., *Nature*, **386**, 671–674 (1997).
29) Ferrara N., Davis-Smyth T., *Endocr. Rev.*, **18**, 4–25 (1997)
30) Shibuya M., Claesson-Welsh L., *Exp. Cell Res.*, **312**, 549–560 (2006).
31) Smith G. P., *Science*, **228**, 1315–1317 (1985).
32) McCafferty J., Griffiths A. D., Winter G., Chiswell D. J., *Nature*, **348**, 552–554 (1990).
33) Marks J. D., Hoogenboom H. R., Bonnert T. P., McCafferty J., Griffiths A. D., Winter G., *J. Mol. Biol.*, **222**, 581–597 (1991).
34) Barbas C. F. 3rd, Kang A. S., Lerner R. A., Benkovic S. J., *Proc. Natl. Acad. Sci. USA*, **88**, 7978–7982 (1991).
35) Vaughan T. J., Williams A. J., Pritchard K., Osbourn J. K., Pope A. R., Earnshaw J. C., McCafferty J., Hodits R. A., Wilton J., Johnson K. S., *Nat. Biotechnol.*, **14**, 309–314 (1996).
36) Coomber D. W., *Methods. Mol. Biol.*, **178**, 133–145 (2002).
37) Goletz S., Christensen P. A., Kristensen P., Blohm D., Tomlinson I., Winter G., Karsten U., *J. Mol. Biol.*, **315**, 1087–1097 (2002).
38) Utoguchi N., Mizuguchi H., Saeki K., Ikeda K., Tsutsumi Y., Nakagawa S., Mayumi T., *Cancer Lett.*, **89**, 7–14 (1995).
39) Okamoto T., Mukai Y., Yoshioka Y., Shibata H., Kawamura M., Yamamoto Y., Nakagawa S., Kamada H., Hayakawa T., Mayumi T., Tsutsumi Y., *Biochem. Biophys. Res. Commun.*, **323**, 583–591 (2004).
40) Rojas G., Almagro J. C., Acevedo B., Gavilondo J. V., *J. Biotechnol.*, **94**, 287–298 (2002).
41) Zhang Z. C., Hu X. J., Yang Q., *Hepatobiliary Pancreat. Dis. Int.*, **3**, 77–81 (2004).

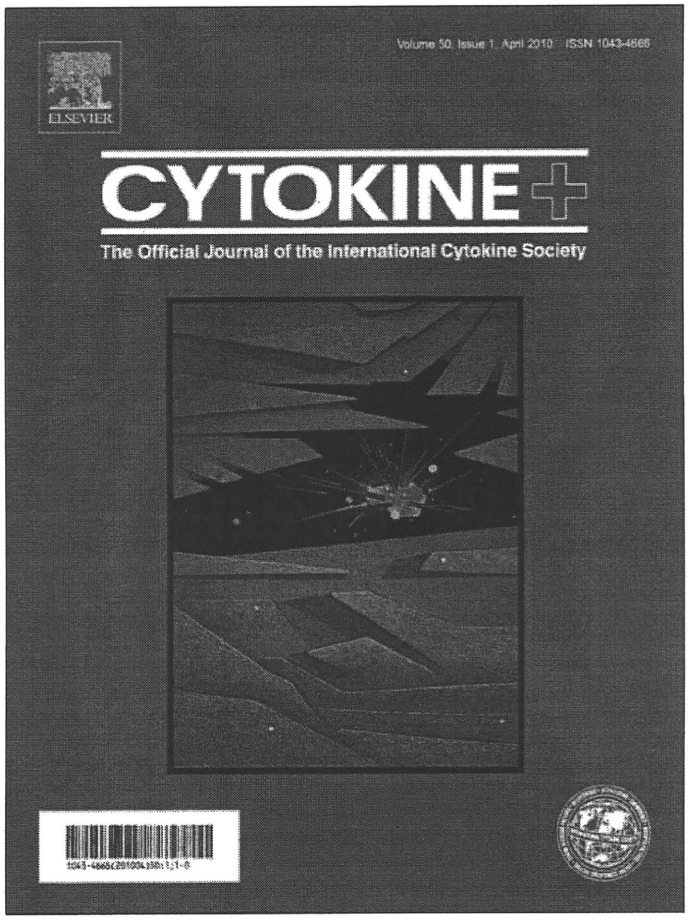

Cytokine 50 (2010) 75–83

Contents lists available at ScienceDirect

Cytokine

journal homepage: www.elsevier.com/locate/issn/10434666

Generation of mouse macrophages expressing membrane-bound TNF variants with selectivity for TNFR1 or TNFR2

Hiroko Shibata [a,b,1], Yasuhiro Abe [a,1], Yasuo Yoshioka [a,c,1], Tetsuya Nomura [a,d], Masaki Sato [a], Hiroyuki Kayamuro [a,d], Tomoyuki Kawara [a,d], Shuhei Arita [a,d], Tsuyoshi Furuya [a,d], Kazuya Nagano [a], Tomoaki Yoshikawa [a,d], Haruhiko Kamada [a,c], Shin-ichi Tsunoda [a,c,d,*], Yasuo Tsutsumi [a,c,d]

[a] National Institute of Biomedical Innovation (NiBio), 7-6-8 Saito-Asagi, Ibaraki, Osaka 567-0085, Japan
[b] National Institute of Health Science (NIHS), Kamiyoga 1-18-1, Setagaya-ku, Tokyo 158-8501, Japan
[c] The Center for Advanced Medical Engineering and Informatics, Osaka University, 1-6 Yamadaoka, Suita, Osaka 565-0871, Japan
[d] Graduate School of Pharmaceutical Sciences, Osaka University, 1-6 Yamadaoka, Suita, Osaka 565-0871, Japan

ARTICLE INFO

Article history:
Received 31 July 2009
Received in revised form 6 November 2009
Accepted 24 November 2009

Keywords:
Transmembrane TNF
TNFR1
TNFR2
Mutant TNF
Lentiviral vector

ABSTRACT

Tumor necrosis factor-alpha (TNF) is expressed on the cell surface as a transmembrane form (tmTNF), that can be released as a soluble form (solTNF) via proteolytic cleavage. These two types of TNF exert their biological functions by binding to one of two TNF receptors, TNFR1 or TNFR2. However, the biological function of tmTNF through these two receptors remains to be determined. Here, we generated macrophages that expressed tmTNF mutants with selectivity for either TNFR1 or TNRF2 as a tool to evaluate signaling through these receptors. Wild-type TNF (wtTNF), TNFR1-selective mutant TNF (mutTNF-R1) or TNFR2-selective mutant TNF (mutTNF-R2) were individually expressed on the TNFR1$^{-/-}$R2$^{-/-}$ mouse macrophages (Mφ) as the tmTNF forms. tm-mutTNF-R1-expressing Mφ exhibited significant selectivity for binding to TNFR1, whereas tm-mutTNF-R2-expressing Mφ only showed a slight selectivity for binding to TNFR2. Signaling by tm-mutTNF-R1-expressing Mφ through the hTNFR2 was weaker than that of tm-wtTNF-expressing Mφ, suggesting that the binding selectivity correlated with functional selectivity. Interestingly, signaling by tm-mutTNF-R2-expressing Mφ through TNFR2 was much stronger than signaling by tm-wtTNF-expressing Mφ, whereas signaling by the corresponding soluble form was weaker than that mediated by wtTNF. These results indicate tmTNF variants might prove useful for the functional analysis of signaling through TNF receptors.

1. Introduction

Tumor necrosis factor alpha (TNF) plays a crucial role in the host defense system [1]. Increased secretion of TNF is involved in the development of autoimmune diseases, such as rheumatoid arthritis (RA) and Crohn's disease [2,3]. Indeed, anti-human TNF antibody and soluble TNF receptor (TNFR), which interfere with the activity of TNF, have been used to treat these diseases, and are expected to be revolutionary therapies due to their excellent therapeutic effects [4]. TNF is primarily produced as a type II transmembrane form (tmTNF) arranged in stable homotrimers [5,6]. A mature, soluble homotrimeric 17-kDa TNF (solTNF) is released from this 26 kDa memTNF *via* proteolytic cleavage by the metalloprotease, TNF converting enzyme (TACE) [7]. Both solTNF and tmTNF induce cell signaling. tmTNF acts through cell–cell contacts to promote juxtacrine signaling, and solTNF acts in a paracrine fashion. The relative contribution of tmTNF and solTNF to overall TNF activity is difficult to elucidate due to the absence of physiologically relevant models. However, evidence for distinct roles for tmTNF and solTNF *in vivo* have been obtained in genetically modified mice. Study of tmTNF knock-in mice revealed that solTNF is required for the development of acute and chronic inflammation, whereas tmTNF supports many processes underlying the development of lymphoid tissue [8]. Mueller et al. also reported that tmTNF has a strong effect upon the course of cellular immune responses *in vivo* and exerts quantitatively and qualitatively distinct functions from solTNF *in vitro* and *in vivo* [9]. Additionally, juxtacrine signaling by tmTNF was shown to be essential for the resolution of inflammation and the maintenance of immunity to the pathogens, *Listeria monocytogenes* and *Mycobacterium tuberculosis* [10–12]. These different functions mediated by the two forms of TNF may help to explain the opposing activities of TNF, such as

* Corresponding author. Address: National Institute of Biomedical Innovation, Laboratory of Pharmaceutical Proteomics, 7-6-8 Saito-Asagi, Ibaraki, Osaka 567-0085, Japan. Tel.: +81 72 639 7014; fax: +81 72 641 9817.
E-mail address: tsunoda@nibio.go.jp (S.-i. Tsunoda).
[1] These authors contributed equally to this work.

1043-4666/$ - see front matter © 2009 Elsevier Ltd. All rights reserved.
doi:10.1016/j.cyto.2009.11.022

its inflammatory and anti-inflammatory effects. However, the factors underlying the different functions of solTNF and tmTNF and the components of the specific signaling cascades induced by the two forms of TNF remain to be elucidated.

solTNF and tmTNF interact with two receptor subtypes, p55 TNF receptor (TNFR1) and p75 TNF receptor (TNFR2) [13], to exert their biological functions. The interaction of solTNF with TNFR and the downstream signaling and functional outcome of that signaling has been extensively studied [14], because signaling by solTNF *via* TNFR1 or TNFR2 can be analyzed *in vitro* using recombinant wild-type TNF, as well as recombinant TNFR1-, and TNFR2-selective mutant TNF (mutTNF). On the other hand, the analysis of tmTNF/TNFR signaling is still poorly understood. tmTNF-expressing cells have previously been reported following transfection into target cells of a TNF gene containing a deletion of the TNF cleavage site [15]. Nanoparticles decorated with solTNF chemically bound to the surface initiate strong TNFR2 responses, and could mimic the bioactivity of tmTNF [16]. However, there are no receptor-selective forms of tmTNF that could be used to analyze tmTNF/TNFR signaling. Moreover, there are few assay systems that can assess the bioactivity of TNF mediated *via* TNFR2 with high sensitively.

In this context, we have used a novel phage-display based screening system to develop TNFR1 or TNFR2-selective mutTNFs to help clarify the biology of TNF/TNFRs interactions. We have already isolated a TNFR1-selective antagonist [17], and both TNFR1 and TNFR2-selective agonists [18]. Additionally, we established a novel cell line hTNFR2/mFas-preadipocyte, which is a simple and highly sensitive, cell death-based assay system for measuring TNFR2-mediated bioactivity [19]. This assay system can assess both solTNF and tmTNF-mediated bioactivity. In this study, we first expressed the TNFR-selective mutTNFs agonists (mutTNF-R1, mutTNF-R2) in TNFR1$^{-/-}$R2$^{-/-}$ macrophages, and we then investigated the possibility of creating TNFR1- and TNFR2-selective tmTNF.

2. Materials and methods

2.1. Cells

The immortalized TNFR1$^{-/-}$R2$^{-/-}$macrophage cell line (DKO Mφ) established from the bone marrow of a TNFR1$^{-/-}$R2$^{-/-}$ mouse was generously provided by Dr. Aggarwal (The University of Texas M.D. Anderson Cancer Center, Houston TX), and cultured in RPMI-1640 medium supplemented with 10% fetal bovine serum (FBS) and 1% antibiotic cocktail (penicillin 10,000 U/ml, streptomycin 10 mg/ml, and amphotericin B 25 μg/ml; Nacalai Tesque, Kyoto, Japan). Human-TNFR2/mouse-Fas-expressing preadipocytes (hTNFR2/mFas-PA) were maintained in Dulbecco's modified Eagle's medium (DMEM; Sigma–Aldrich, Inc., Tokyo, Japan) with 10% FBS, 1% antibiotic cocktail, and 5 μg/ml blasticidin (Bsd) (Invitrogen Corp., Carlsbad, CA). hTNFR2/mFas-PA cells express a chimeric receptor derived from the extracellular and transmembrane domain of human TNFR2 fused to the intracellular domain of mouse Fas [19]. 293T cells and HeLaP4 cells were cultured in DMEM with 10% FBS and 1% antibiotic cocktail. HEp-2 cells are a human laryngeal squamous cell carcinoma cell line, and were cultured in RPMI-1640 medium supplemented with 10% FBS and 1% antibiotic cocktail.

2.2. Surface plasmon resonance (SPR) assay

The binding kinetics of wtTNF, mutTNF-R1 and mutTNF-R2 were analyzed by the SPR technique using a BIAcore 3000 (BIAcore®, GE Healthcare, Buckinghamshire, UK). Human TNFR1 or human TNFR2 Fc chimeras (R&D systems, Minneapolis, MN) were diluted to 50 μg/ml in 10 mM sodium acetate buffer (pH 4.5). TNFRs were immobilized on a CM5 sensor chip, which resulted in an increase of 3000–3500 resonance units (RU). During the association phase, TNFs diluted in running buffer (HBS-EP) at 156.8, 52.3 or 17.4 nM were individually passed over the immobilized TNFRs at a flow rate of 20 μl/min. During the dissociation phase, HBS-EP buffer was applied to the sensor chip at a flow rate of 20 μl/min. The data were analyzed with BIAEVALUATION 3.0 software (BIAcore®) using a 1:1 binding model.

2.3. Cytotoxicity assays

HEp-2 cells were cultured in 96-well plates (4×10^4 cells/well) in a serial dilution of human TNF (Peprotech, Rocky Hill, NJ) or mutTNFs with 100 μg/ml cycloheximide. After incubation for 18 h, cell survival was determined using the methylene blue assay as described previously [17]. hTNFR2/mFas-PA were seeded onto 96-well plates at a density of 1.5×10^4 cells/well in culture medium. Serial dilutions of human TNF or paraformaldehyde-fixed Mφ cells were prepared in DMEM containing 1 μg/ml cycloheximide, and added to each well. After 48 h, cell viability was measured using the WST-assay kit (Nacalai Tesque) according to the manufacturer's instructions.

2.4. Construction of a self-inactivating (SIN) lentiviral vector

Vectors were constructed using standard cloning procedures. A DNA fragment encoding the precursor signal of human TNF was amplified by polymerase chain reaction (PCR) with the following primer pairs : forward primer-1 (5′-GAT TTC GAT ACG TAC GGA AGC TTC GTC GAC ATT AAT TAA GGA CAC CAT GAG CAC TGA AAG CAT GAT CCG GGA CGT GGA GCT GGC CGA GGA GG-3′) containing a SalI site at the 5′-end, reverse primer-1 (5′-AGA GGC TGA GGA ACA AGC ACC GCC TGG AGC CCT GGG GCC CCC CTG TCT TCT TGG GGA GCG CCT CCT CGG CCA GCT CCA CGT CCC GGA TCA-3′), forward primer-2 (5′-GCT CCA GGC GGT GCT TGT TCC TCA GCC TCT TCT CCT TCC TGA TCG TGG CAG GCG CCA CCA CGC TCT TCT GCC TGC TGC ACT TTG GAG TGA-3′), and reverse primer-2 (5′-TGC CTG GGC CAG AGG GCG CGG CCG CGA GAT CTC TGG GGA ACT CTT CCC TCT GGG GGC CGA TCA CTC CAA AGT GCA GCA GGC AGA AGA GCG-3′) containing BglII site at the 5′-end. The resulting amplified fragment was subcloned into the pY02 vector to generate pY02-preTNF. DNA fragments encoding non-cleavable wild-type human TNF (tm-wtTNFΔ1–12) (Fig. 2a), TNFR1-selective mutant TNF (tm-mutTNF-R1Δ1–12), and TNFR2-selective mutant TNF (tm-mutTNF-R2Δ1–12) which were generated by deleting amino acids 1–12 in the N-terminal part of TNF, were amplified by PCR from wtTNF, mutTNF-R1, and mutTNF-R2 respectively with the following primer pairs : forward primer-3 (5′-AGT GAT CGG CCC CCA GAG GGA AGC TTA GAT CTC TCT CTA ATC AGC CCT CTG GCC CAG GCA GTA GCC CAT GTT GTA GCA AAC CCT CAAG-3′) containing a BglII site at the 5′-end, and reverse primer-3 (5′-GGT TGG ATG TTC GTC CTC CGC GGC CGC CTA ACT AGT TCA CAG GGC AAT GAT CCC AAA GTA GAC CTG-3′) containing a NotI site at the 5′-end. These fragments were cloned into the pY02-preTNF vector. Then, fragments of tm-wtTNFΔ1–12, tm-mutTNF-R1Δ1–12, and tm-mutTNF-R2Δ1–12 were cloned between the SalI and NotI sites of the SIN vector construct, generating CSII-EF-tm-wtTNF-IRES-GFP, CSII-EF-tm-mutTNF-R1-IRES-GFP, and CSII-EF-tm-mutTNF-R2-IRES-GFP, respectively.

2.5. Preparation of lentiviral vectors

Lentiviral vectors were prepared as previously described [20,21]. In brief, 293T cells were transfected by the calcium phosphate method with three plasmids: packaging construct (pCAG-HIVgp), VSV-G and Rev expressing construct (pCMV-VSV-G-RSV-Rev) and

the SIN vector constructs (CSII-EF-tm-wtTNF-IRES-rhGFP, CSII-EF-tm-mutTNF-R1-IRES-rhGFP or CSII-EF-tm-mutTNF-R2-IRES-rhGFP) (Fig. 2b). Two days after transfection, the conditioned medium was collected and the virus was concentrated by ultracentrifugation at 50,000*g* for 2 h at 20 °C. The pelleted virus was re-suspended in Hank's balanced salt solution (GIBCO BRL, Paisley, UK). Vector titers were determined by measuring the infectivity of HeLaP4 cells with serial dilutions of vector stocks using flow cytometric analysis (FCM) for GFP-positive cells.

2.6. Creation of membrane-bound TNF expressing cells

To prepare tmTNF-expressing cells, DKO Mφ (1×10^3 cells/well) cells were transfected with each lentiviral vector (tm-wtTNF, tm-mutTNF-R1 or tm-mutTNF-R2) at a multiplicity of infection (MOI) of 160 in 96-well plates. Infected cells were cultured until reaching 1×10^7 cells. IRES-driven GFP-positive cells were single-cell-sorted by FACSVantage™ (BD Biosciences, Franklin Lakes, NJ), and cultured in conditioned medium from DKO Mφ cells. After blocking Fc receptors with anti-mouse CD16/32 (eBioscience, San Diego, CA), the expression of tmTNF on monoclonal cell lines was detected by staining with Phycoerythrin-conjugated anti-human TNF antibody (clone MAb11, eBioscience) at 0.5 μg/5×10^5 cells for 30 min on ice. Subsequently, the cells were washed with 1% FBS/PBS and re-suspended in 500 μl of 4% paraformaldehyde. GFP or phycoerythrin fluorescence was analyzed using FCM by FACSCalibur™. Monoclonal cell lines stably expressing tmTNF or its mutants and GFP (tmTNF-expressing Mφ, tm-wtTNF Mφ, tm-mutTNF-R1 Mφ, or tm-mutTNF-R2 Mφ) were used for the following experiments.

2.7. Measurement of receptor binding activity by FCM

To detect the binding of soluble human TNFR1 (shTNFR1) or TNFR2 (shTNFR2) to tmTNF on Mφ cell lines, shTNFR1- or shTNFR2-Fc chimera were labeled with R-phycoerythrin by Zenon™ Human IgG Labeling Kits (Invitrogen Corp.) according to the manufacturer's procedure. Briefly, 10 μl of shTNFR1- or shTNFR2-Fc chimera (250 μg/ml) (R&D systems) was incubated with 5 μl labeling reagent for 5 min at room temperature, and 5 μl blocking reagent was added to each reaction solution. After incubation for 5 min at room temperature, 4 μl each reaction solution was added to 5×10^5 cells/tube which were pretreated with mouse Fc block. After incubation for 30 min on ice, the cells were washed with 1% FBS/PBS, and then suspended in 500 μl of 0.4% paraformaldehyde.

3. Results and discussion

An understanding of the bioactivity of tmTNF is key to a better understanding of the overall function of TNF and TNF receptors. The relative contribution of signaling by tmTNF through the TNFR1 and TNFR2 receptors is unclear, as it is difficult to monitor the specific activation of these two receptors in response to tmTNF. To address this problem, we established macrophage cell lines expressing TNFR-selective mutant TNFs (tmTNF-R1 or tmTNF-R2) on the cell surface.

First, to assess the receptor selectivity of soluble mutTNF-R1 or R2 (sol-mutTNF-R1 or R2), which we previously created using a phage display system [18], we measured human TNFR1-mediated bioactivities of sol-mutTNFs on HEp-2 cells and human TNFR2-mediated bioactivities on hTNFR2/mFas-PA cells (Fig. 1a and Table 1). The binding affinity and kinetic parameters of these mutant TNFs for each TNF receptor were also measured using a Surface plasmon resonance assay (Fig. 1b and Table 1). We observed that both the bioactivity and binding affinity of sol-mutTNF-R1 for hTNFR1 were equivalent to those of sol-wtTNF, whereas the activity and affinity of sol-mut-TNF-R1 for hTNFR2 were decreased to less than 0.2% and 8%, respectively, of the values observed with sol-wtTNF. Although the bioactivity of sol-mutTNF-R2 mediated via hTNFR2 was only 16% of that of sol-wtTNF, the binding affinity of sol-mutTNF-R2 for human TNFR2 was about 1.5 times higher than that of sol-wtTNF. The bioactivity and binding affinity of sol-mutTNF-R2 for hTNFR1 were decreased to less than 0.1% and 3%, respectively, of the corresponding values for sol-wtTNF. Interestingly, the kinetic parameters, k_{on} and k_{off}, of the sol-mutTNFs for the TNF receptors tended to be higher than those of sol-wtTNF, indicating rapid association/dissociation interaction. From these data, we confirmed a significant TNFR-selectivity of sol-mutTNF-R1 and sol-mutTNF-R2. Therefore, we attempted to create the corresponding TNFR-selective tmTNFs using these sol-mutTNFs.

To express only tmTNF on the cell surface, the recombinant genes corresponding to each sol-TNF mutant, each encoding a protein with an additional twelve amino acid deletion from the N-terminus, were subcloned into lentiviral vectors (Fig. 2a and b). The resulting recombinant lentiviral vectors were transduced into $TNFR1^{-/-}R2^{-/-}$ macrophages (DKO Mφ). As previously reported, the deletion of the first 12 amino acids from the N-terminus of TNF, including the entire TACE cleavage site, leads to the expression of only the tmTNF form, and not the soluble form [15,22]. Since the SIN vector also comprises a GFP expression cassette, GFP expression was visible in all three cell lines: wtTNF-expressing DKO Mφ (tm-wtTNF Mφ), mutTNF-R1 expressing DKO Mφ (tm-mutTNF-R1 Mφ), and mutTNF-R2 expressing DKO Mφ (tm-mutTNF-R2 Mφ) (Fig. 2c). We next verified the expression of TNF on single sorted cells using FCM analysis. We observed significant expression of TNF on tm-wtTNF Mφ (Fig. 3a). The mean fluorescence intensity (MFI) of tm-mutTNF-R1 Mφ and tm-mutTNF-R2 Mφ was lower than that of tm-wtTNF Mφ (Fig. 3b). Since the expression level of GFP on tm-mutTNF-R1 Mφ and tm-mutTNF-R2 Mφ was lower than that on tm-wtTNF Mφ (Fig. 2c), the expression level of TNF on these cells might also be lower than that on tm-wtTNF Mφ.

Next, the affinity of each cell-surface expressed tmTNF for soluble TNF receptors was measured by FCM analysis (Fig. 4a), and receptor selectivity was estimated (Fig. 4b and c). We observed that both soluble TNFR1 and TNFR2 Fc chimeras bound to tm-wtTNF Mφ, although TNFR2 bound to tm-wtTNF Mφ with an affinity approximately twofold stronger than that of TNFR1 (Fig. 4b). Although the affinity of tm-mutTNF-R1 Mφ for TNFR1 was 50% that of tm-wtTNF Mφ, the affinity of tm-mutTNF-R1 Mφ for TNFR2 was greatly decreased and the ratio of selectivity of tm-mutTNF-R1 Mφ for TNFR1 over TNFR2 (R1/R2 of MFI) was approximately three times that of tm-wtTNF Mφ (Fig. 4b and c). Therefore, the expression of mutTNF-R1 on the cell surface as the tmTNF form demonstrates TNFR1 selectivity, as does its soluble form. On the other hand, the affinity of TNFR1 and TNFR2 for tm-mutTNF-R2 Mφ was weaker than their affinity for tm-wtTNF Mφ (Fig. 4a and b). Additionally, the ratio of selectivity of tm-mutTNF-R2 Mφ for TNFR1 over TNFR2 was similar to that of tm-wtTNF Mφ, indicating little selectivity for TNFR2 in contrast to what was observed for sol-mutTNF-R2 (Fig. 4c). We next evaluated the bioactivity of these tmTNFs via hTNFR2, by assessing the cytotoxicity of these tmTNFs on hTNFR2/mFas-PA cells, which express the hTNFR2/mFas chimeric receptor (Fig. 5). As previously reported, a cytotoxicity assay using hTNFR2/mFas-PA cells is a simple and highly sensitive assay system for determining TNFR2-mediated activity. DKO Mφ expressing each type of tmTNF (effector cell) were fixed with paraformaldehyde, and co-cultured with hTNFR2/mFas-PA cells (target cell). The viability of the target cells decreased significantly and in a dose-dependent manner

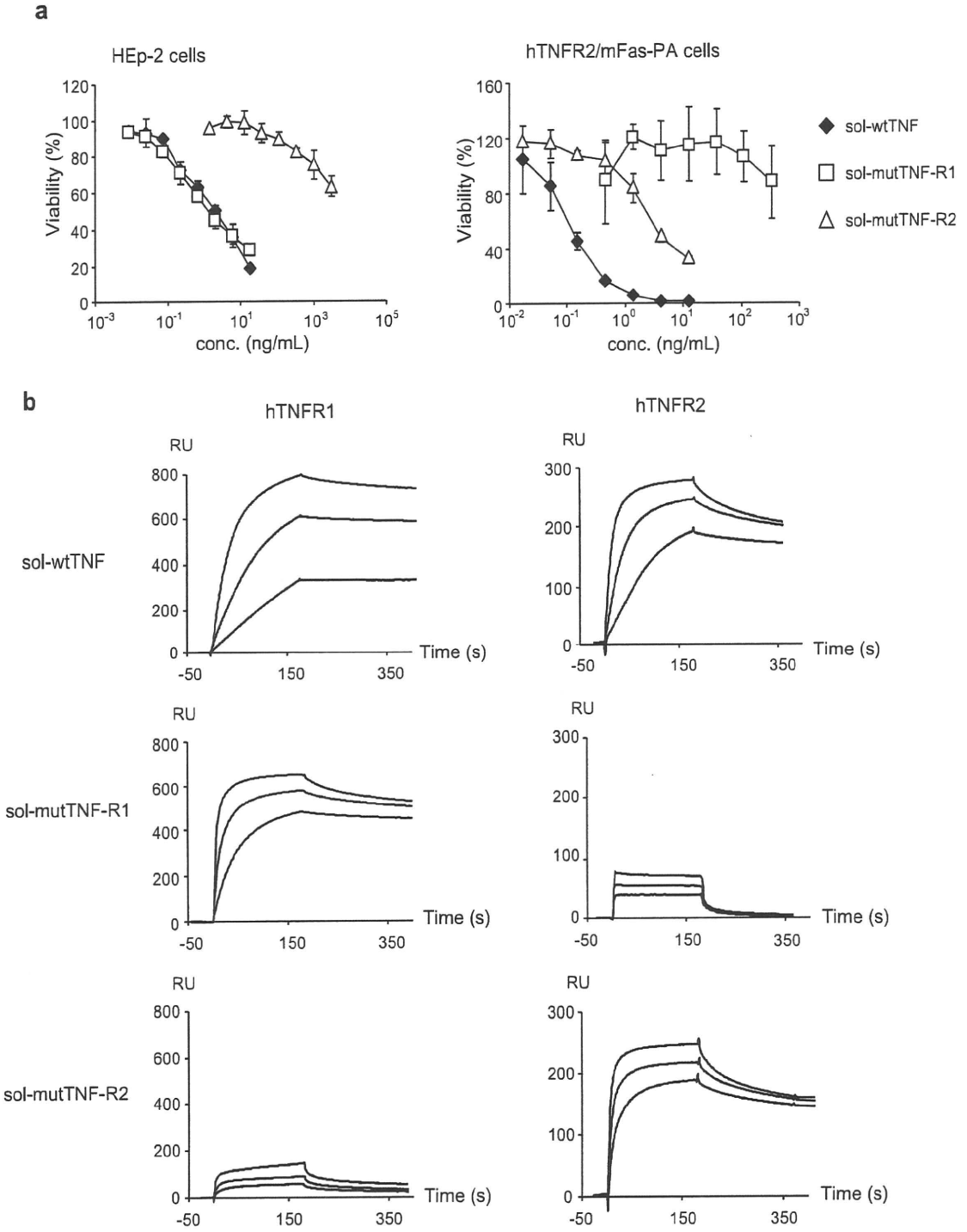

Fig. 1. Bioactivity and binding of sol-wtTNF, sol-mutTNF-R1, and sol-muTNF-R2 to TNFRs. (a) HEp-2 cells or hTNFR2/Fas-PA cells were used for measuring TNFR1-mediated or TNFR2-mediated bioactivity respectively. HEp-2 cells were cultured in serial dilutions of sol-wtTNF, sol-mutTNF-R1, and sol-mutTNF-R2 with 100 μg/ml cycloheximide for 18 h. hTNFR2/Fas-PA cells were also cultured in serial dilutions of sol-TNFs with 1 μg/ml cycloheximide for 48 h. Cell viability was determined using the methylene blue assay for HEp-2 cells, and the WST-8 assay for hTNFR2/Fas-PA cells. (b) The binding kinetics of sol-TNFs to immobilized TNFRs were analyzed using the surface plasmon resonance (SPR) technique. TNFRs were immobilized to a sensor chip CM5, which resulted in an increase of 3000–3500 resonance units (RU). The amount of protein bound to the surface was recorded in RU. Duplicate injections of 156.8, 52.3, or 17.4 nM sol-TNFs were passed over the immobilized TNFRs at a flow rate of 20 μl/min. The sensorgrams shown were normalized by subtracting the control surface sensorgram.

when exposed to an increasing *E*(effector)/*T*(target) cell ratio of tm-wtTNF Mφ compared to exposure to the control DKO Mφ. These results suggest that tmTNF induced death of these cells in a dose-dependent manner via signaling through the TNFR2/mFas chimera expressed on the target cell surface. The bioactivity of tm-mutTNF-R1 Mφ was lower than that of tm-wtTNF Mφ in

Table 1
Amino acid sequence, bioactivity, and kinetic parameters of mutTNFs.

Human TNFs	Amino acids sequence						Bioactivity EC50 (nM)		Binding property					
									TNFR1			TNFR2		
	29	31	32	145	146	147	HEp-2	hTNFR2/ mFas-PA	k_{on} $(M^{-1}\,S^{-1})^a$	k_{off} $(s^{-1})^b$	k_d (nM)^c	k_{on} $(M^{-1}\,S^{-1})^a$	k_{off} $(S^{-1})^b$	k_d (nM)^c
sol-wtTNF	L	R	R	A	E	S	1.9 (100%)	0.5 (100%)	2.1×10^5	1.4×10^{-4}	0.68 (100%)	1.1×10^6	7.8×10^{-4}	0.70 (100%)
sol-mutTNF-R1	K	A	G	A	S	T	1.5 (128%)	>300 (<0.2%)	6.5×10^5	4.7×10^{-4}	0.73 (93%)	5.8×10^6	522.0×10^{-4}	9.0 (8%)
sol-mutTNF-R2	L	R	R	R	E	T	>3000 (<0.1%)	3.1 (16%)	1.8×10^5	36.1×10^{-4}	20.2 (3%)	3.1×10^6	15.4×10^{-4}	0.49 (144%)

Kinetic parameters for each TNF were calculated by from the respective sensorgrams by BIA evaluation 3.0 software. Value in parenthesis shows the relative bioactivity or relative binding affinity (%).

[a] k_{on} is association kinetic constant.

[b] k_{off} is dissociation kinetic constant.

[c] k_d (equilibrium dissociation constant) denotes binding affinity.

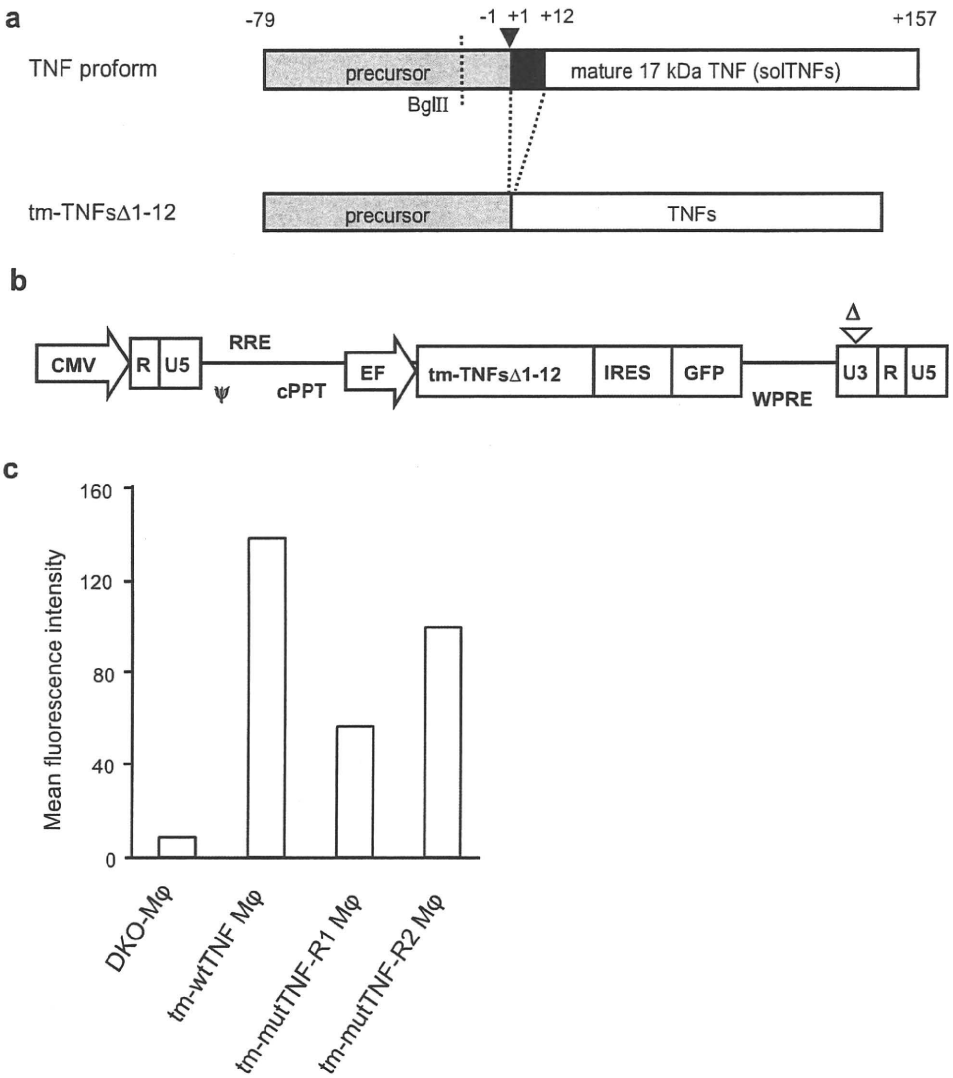

Fig. 2. Schematic representation of the tmTNF forms and the construction of the lentiviral vector. (a) Schematic representation of non-cleavable human TNFs (tm-TNFsΔ1–12). An inverted filled triangle shows the cleavage site. Closed bar, amino acids 1–12, indicates the deleted region. (b) Schematic representation of self-inactivating (SIN) LV plasmid (CSII-EF-tm-TNFsΔ1–12-IRES-GFP). CMV: cytomegalovirus promoter, ψ: packaging signal, RRE: rev responsive element, cPPT: central polypurine tract, IRES: Encephalomyocarditis virus internal ribosomal entry site, Bsd: Blasticidin, WPRE: woodchuck hepatitis virus posttranscriptional regulatory element. Δ: deletion of 133 bp in the U3 region of the 3′ long terminal repeat. (c) Expression of GFP on each cell was analyzed by FCM, and the mean fluorescence intensity of each cell is shown.

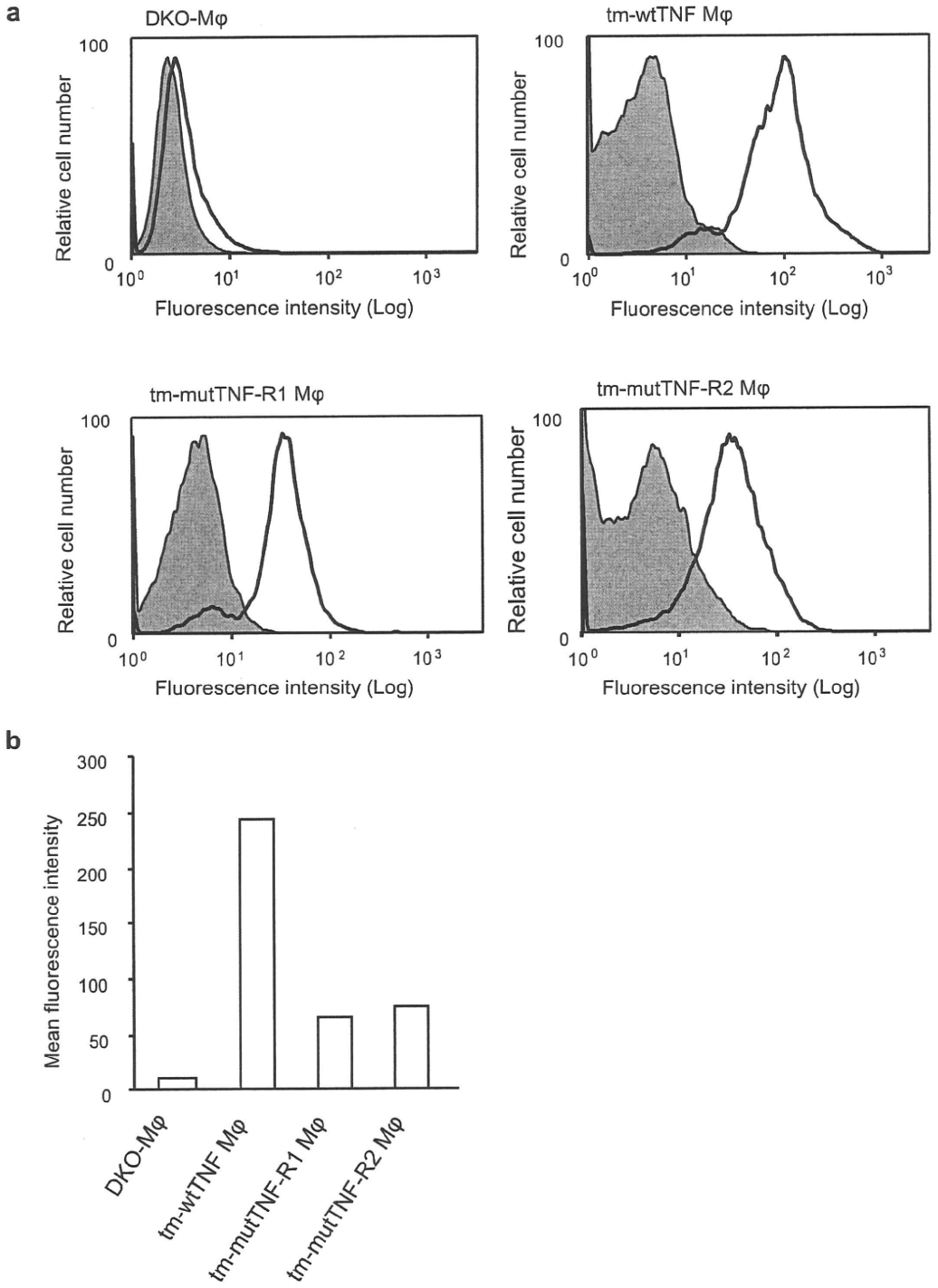

Fig. 3. The expression of TNF as the transmembrane form on tm-TNFs Mφ. (a) Expression of TNF on each cell was analyzed by FCM using PE-conjugated anti-hTNF monoclonal antibody (open histograms) or PE-conjugated isotype control antibody (shaded histograms). (b) The mean fluorescence intensity of each cell is shown.

this assay, which correlates with the results observed when studying its soluble form in Table 1. Interestingly, tm-mutTNF-R2 Mφ was more cytotoxic than tm-wtTNF Mφ, whereas the cytotoxicity of sol-mutTNF-R2 was only 16% of that of sol-wtTNF in this assay.

In this study, we have established the selectivity of tm-mutTNF-R1 Mφ for binding to TNFR1, although we need to measure the precise expression level of TNF in each cell. In addition, FCM analysis suggested that tm-mutTNF-R2 Mφ have a lower affinity for both TNFRs than do tm-wtTNF Mφ, and that they exhibit little selectivity

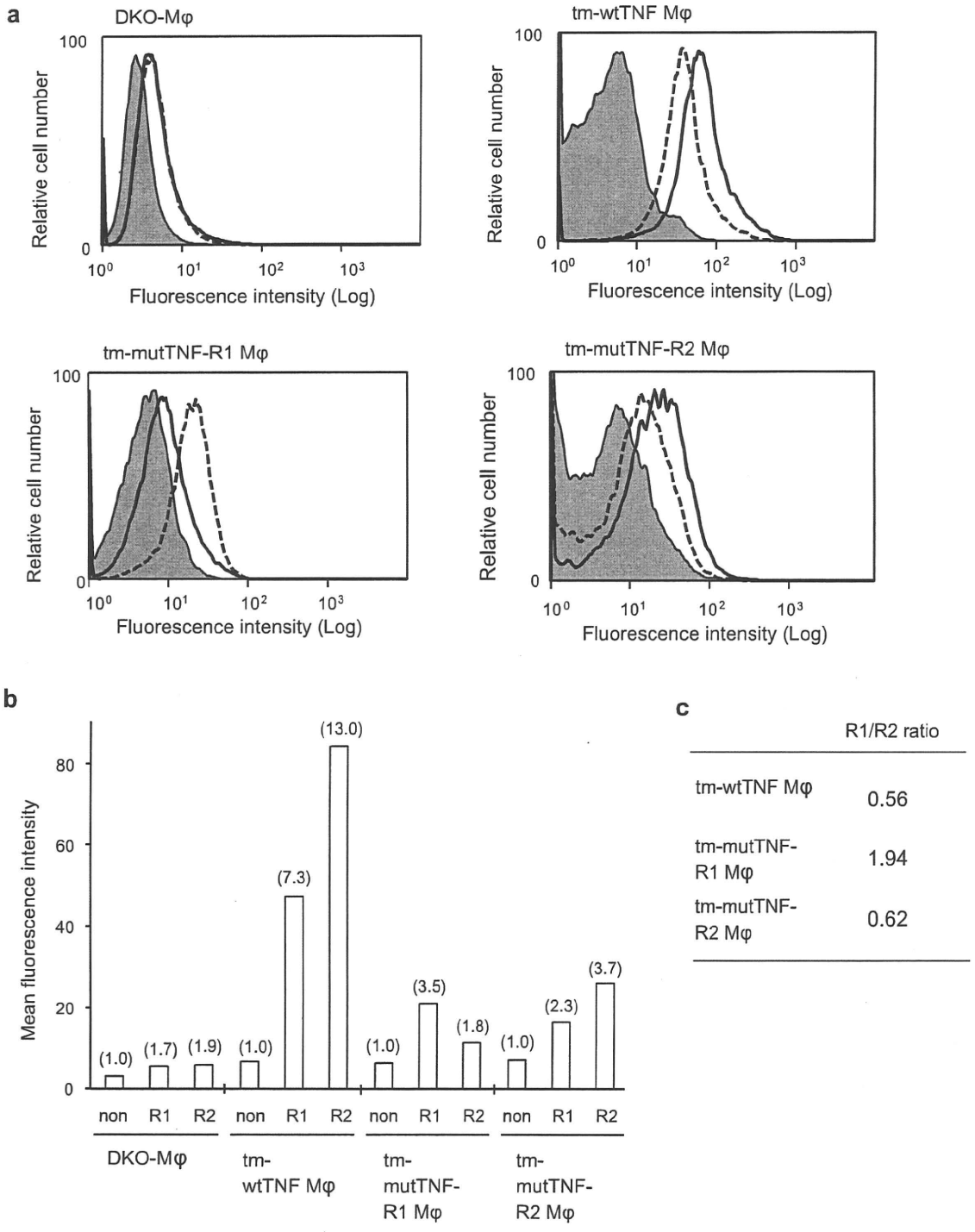

c

	R1/R2 ratio
tm-wtTNF Mφ	0.56
tm-mutTNF-R1 Mφ	1.94
tm-mutTNF-R2 Mφ	0.62

Fig. 4. The affinity of tm-TNFs Mφ for soluble TNF-receptors. (a) The binding of each tmTNF to solTNFR1 (dashed lines) or solTNFR2 (solid lines) was analyzed by FCM analysis. DKO Mφ, tm-wtTNF Mφ, tm-mutTNF-R1 Mφ, and tm-mutTNF-R2 Mφ were stained with solTNFR1- or solTNFR2-Fc chimera that was labeled with PE-conjugated Fab fragment of anti-human Fc antibody. Shaded histograms show non-stained cells. (b) Mean fluorescence intensity of each cells is shown. (c) Values in parenthesis indicate the relative intensity against non-treated cells in each cell line.

for TNFR2. In this report, we established macrophage cell lines expressing only tmTNF, and not solTNF, owing to the deletion of the first 12 amino acids (Δ1–12) of each TNF mutant. Although most studies have made use of the Δ1–12 TNF mutation for the investigation of tmTNF activity, the bioactivity of the resulting non-cleavable tmTNF is reported to be reduced compared to

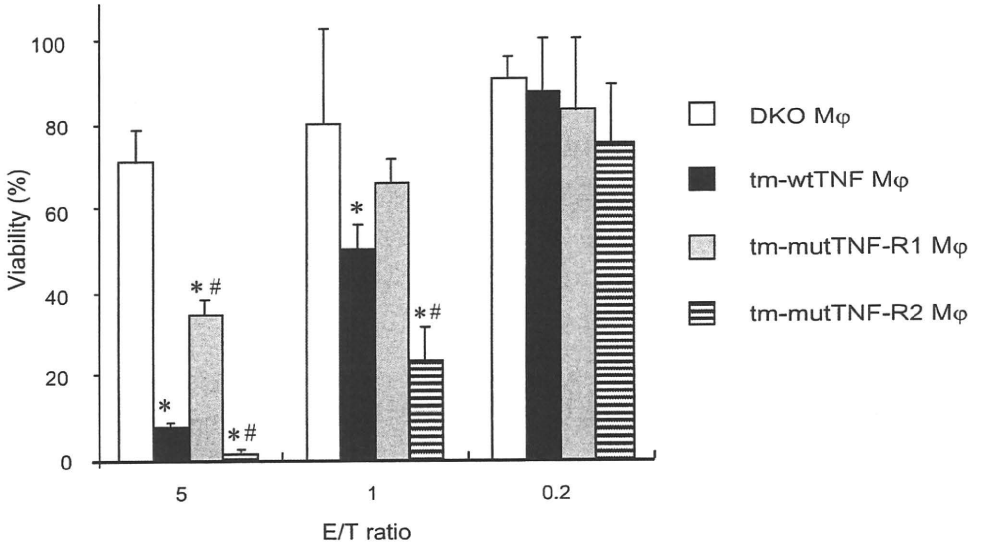

Fig. 5. tm-mutTNF-R2 Mφ induced death of hTNFR2/mFas-PA cells. hTNFR2/mFas-PA cells were co-incubated with paraformaldehyde-fixed DKO Mφ (open bars), tm-wtTNF Mφ (filled bards), tm-mutTNF-R1 Mφ (shaded bards), or tm-mutTNF-R2 Mφ (stiped bards) at an effector/target (E/T) ratio of 5:1, 1:1, or 0.2:1 in the presence of cycloheximide (1 μg/ml). After 48 h, cell viability was measured by the WST-8 Assay. Data were expressed as mean values ± SD of triplicate measurements and analyzed by one-way ANOVA (Dunnett's test). $^{*}p < 0.05$: compared to DKO Mφ, $^{\#}p < 0.05$: compared to tm-wtTNF Mφ.

wild-type tmTNF, whereas a tmTNF mutant containing a Δ1–9 K11E mutation exhibited normal cell-surface expression and a bioactivity similar to the wild-type [22]. Therefore, use of this latter deletion backbone may allow greater TNFR-selectivity in Mφ engineered to express tm-mutTNF-R2, and may generate superior TNFR-selective tmTNF-expressing cells.

As described earlier, tmTNF and solTNF have distinct roles or functions in normal and pathological conditions [8]. Furthermore, it is also believed that TNFR2 can only be fully activated by tmTNF [23]. Although the mechanisms underlying these effects are poorly understood, the half lives of the individual ligand/receptor complexes may contribute to the differential activity of tmTNF and solTNF [23]. Krippner-Heidenreich et al. reported that the dissociation rate constant of the cell surface binding of tmTNF to TNFR2 is much lower than that of the binding of solTNF to the same receptor, indicating that tmTNF dissociates much less readily from TNFR2 [24]. Thus, the bioactivity imparted by the interaction of the ligand/receptor pair is dependent upon various binding parameters (binding affinity, association or dissociation rate constant). We have shown here that tm-mutTNF-R2 Mφ exhibit greater cytotoxicity on hTNFR2/mFas-PA cells than do tm-wtTNF Mφ, whereas the cytotoxicity of sol-mutTNF-R2 was lower than that of sol-wtTNF. We assume that the dissociation rate constant of the binding of mutTNF-R2 to immobilized TNFR2 or TNFR2 on the cell surface might be reduced to a level similar to that of tm-wtTNF Mφ upon conversion of the soluble form to the transmembrane form. As such, the threefold higher association rate constant of the interaction of TNFR2 with sol-mutTNF-R2 than that of TNFR2 with sol-wtTNF (Table 1) might explain the strong bioactivity on hTNFR2/mFas-PA cells.

The affinity between a ligand and its receptor is determined by an equilibrium between the rates of association and dissociation, and is determined inherently. Therefore, expression of sol-mutTNFs with selectivity for each TNFR as the corresponding tmTNF forms on the cell surface, may alter the selectivity for the TNFRs. We plan to carry out more detailed analyses of the variant tmTNFs, such as measurement of their expression, their precise affinity for TNFR1 or R2, and their activity mediated through binding and signaling through TNFR1. Eventually, these tmTNFs, tm-mutTNF-R1 and R2 Mφ may prove useful for functional analysis or signal analysis of TNF receptors.

Acknowledgments

This study was supported in part by some Grants-in-Aid for Scientific Research from the Ministry of Education, Culture, Sports, Science and Technology of Japan, and in part by some Grants-in-Aid for Scientific Research from Japan Society for the Promotion of Science (JSPS). And this study was also supported in part by some Health Labour Sciences Research Grants from the Ministry of Health, Labor and Welfare of Japan, and in part by Health Sciences Research Grants for Research on Publicly Essential Drugs and Medical Devices from the Japan Health Sciences Foundation, in part by The Nagai Foundation Tokyo.

References

[1] Aggarwal BB. Signalling pathways of the TNF superfamily: a double-edged sword. Nat Rev Immunol 2003;3:745–56.
[2] Beutler B. Autoimmunity and apoptosis: the Crohn's connection. Immunity 2001;15:5–14.
[3] Feldmann M, Maini RN. Anti-TNF alpha therapy of rheumatoid arthritis: what have we learned? Annu Rev Immunol 2001;19:163–96.
[4] Feldmann M. Development of anti-TNF therapy for rheumatoid arthritis. Nat Rev Immunol 2002;2:364–71.
[5] Kriegler M, Perez C, DeFay K, Albert I, Lu SD. A novel form of TNF/cachectin is a cell surface cytotoxic transmembrane protein: ramifications for the complex physiology of TNF. Cell 1988;53:45–53.
[6] Tang P, Hung MC, Klostergaard J. Human pro-tumor necrosis factor is a homotrimer. Biochemistry 1996;35:8216–25.
[7] Black RA, Rauch CT, Kozlosky CJ, Peschon JJ, Slack JL, Wolfson MF, et al. A metalloproteinase disintegrin that releases tumour-necrosis factor-alpha from cells. Nature 1997;385:729–33.
[8] Ruuls SR, Hoek RM, Ngo VN, McNeil T, Lucian LA, Janatpour MJ, et al. Membrane-bound TNF supports secondary lymphoid organ structure but is subservient to secreted TNF in driving autoimmune inflammation. Immunity 2001;15:533–43.
[9] Mueller C, Corazza N, Trachsel-Loseth S, Eugster HP, Buhler-Jungo M, Brunner T, et al. Noncleavable transmembrane mouse tumor necrosis factor-alpha (TNFalpha) mediates effects distinct from those of wild-type TNFalpha in vitro and in vivo. J Biol Chem 1999;274:38112–8.
[10] Olleros ML, Guler R, Vesin D, Parapanov R, Marchal G, Martinez-Soria E, et al. Contribution of transmembrane tumor necrosis factor to host defense against Mycobacterium bovis bacillus Calmette-guerin and Mycobacterium tuberculosis infections. Am J Pathol 2005;166:1109–20.
[11] Saunders BM, Tran S, Ruuls S, Sedgwick JD, Briscoe H, Britton WJ. Transmembrane TNF is sufficient to initiate cell migration and granuloma formation and provide acute, but not long-term, control of Mycobacterium tuberculosis infection. J Immunol 2005;174:4852–9.

[12] Torres D, Janot L, Quesniaux VF, Grivennikov SI, Maillet I, Sedgwick JD. Membrane tumor necrosis factor confers partial protection to Listeria infection. Am J Pathol 2005;167:1677–87.
[13] Aggarwal BB, Eessalu TE, Hass PE. Characterization of receptors for human tumour necrosis factor and their regulation by gamma-interferon. Nature 1985;318:665–7.
[14] Micheau O, Tschopp J. Induction of TNF receptor I-mediated apoptosis via two sequential signaling complexes. Cell 2003;114:181–90.
[15] Perez C, Albert I, DeFay K, Zachariades N, Gooding L, Kriegler M. A nonsecretable cell surface mutant of tumor necrosis factor (TNF) kills by cell-to-cell contact. Cell 1990;63:251–8.
[16] Bryde S, Grunwald I, Hammer A, Krippner-Heidenreich A, Schiestel T, Brunner H, et al. Tumor necrosis factor (TNF)-functionalized nanostructured particles for the stimulation of membrane TNF-specific cell responses. Bioconjug Chem 2005;16:1459–67.
[17] Shibata H, Yoshioka Y, Ohkawa A, Minowa K, Mukai Y, Abe Y, et al. Creation and X-ray structure analysis of the tumor necrosis factor receptor-1-selective mutant of a tumor necrosis factor-alpha antagonist. J Biol Chem 2008;283:998–1007.
[18] Mukai Y, Shibata H, Nakamura T, Yoshioka Y, Abe Y, Nomura T, et al. Structure-function relationship of tumor necrosis factor (TNF) and its receptor interaction based on 3D structural analysis of a fully active TNFR1-selective TNF mutant. J Mol Biol 2009;385:1221–9.
[19] Abe Y, Yoshikawa T, Kamada H, Shibata H, Nomura T, Minowa K, et al. Simple and highly sensitive assay system for TNFR2-mediated soluble- and transmembrane-TNF activity. J Immunol Methods 2008;335:71–8.
[20] Katayama K, Wada K, Miyoshi H, Ohashi K, Tachibana M, Furuki R, et al. RNA interfering approach for clarifying the PPARgamma pathway using lentiviral vector expressing short hairpin RNA. FEBS Lett 2004;560:178–82.
[21] Miyoshi H, Smith KA, Mosier DE, Verma IM, Torbett BE. Transduction of human CD34+ cells that mediate long-term engraftment of NOD/SCID mice by HIV vectors. Science 1999;283:682–6.
[22] Decoster E, Vanhaesebroeck B, Vandenabeele P, Grooten J, Fiers W. Generation and biological characterization of membrane-bound, uncleavable murine tumor necrosis factor. J Biol Chem 1995;270:18473–8.
[23] Grell M, Douni E, Wajant H, Lohden M, Clauss M, Maxeiner B, et al. The transmembrane form of tumor necrosis factor is the prime activating ligand of the 80 kDa tumor necrosis factor receptor. Cell 1995;83:793–802.
[24] Krippner-Heidenreich A, Tubing F, Bryde S, Willi S, Zimmermann G, Scheurich P. Control of receptor-induced signaling complex formation by the kinetics of ligand/receptor interaction. J Biol Chem 2002;277:44155–63.

National Institute of Biomedical Innovation (NiBio)[1]; Graduate School of Pharmaceutical Sciences[2], Osaka University; The Center for Advanced Medical Engineering and Informatics[3], Osaka University, Osaka, Japan

Creation of an improved mutant TNF with TNFR1-selectivity and antagonistic activity by phage display technology

T. NOMURA[1,2*], Y. ABE[1*], H. KAMADA[1,3], M. INOUE[1], T. KAWARA[1,2], S. ARITA[1,2], T. FURUYA[1,2], K. MINOWA[1], Y. YOSHIOKA[2,3], H. SHIBATA[1], H. KAYAMURO[1,2], T. YAMASHITA[1,2], K. NAGANO[1], T. YOSHIKAWA[1,2], Y. MUKAI[2], S. NAKAGAWA[2,3], S. TSUNODA[1,2,3], Y. TSUTSUMI[1,2,3]

Received August 7, 2009, accepted August 14, 2009

Shin-ichi Tsunoda, Ph.D., Laboratory of Pharmaceutical Proteomics, National Institute of Biomedical Innovation, 7-6-8 Saito-Asagi, Ibaraki, Osaka 567-0085, Japan
tsunoda@nibio.go.jp
**These authors contributed equally to the work.*

Pharmazie 65: 93–96 (2010) *doi: 10.1691/ph.2010.9265*

Tumor necrosis factor-α (TNF), which binds two types of TNF receptors (TNFR1 and TNFR2), regulates the onset and exacerbation of autoimmune diseases such as rheumatoid arthritis and Crohn's disease. In particular, TNFR1-mediated signals are predominantly related to the induction of inflammatory responses. We have previously generated a TNFR1-selective antagonistic TNF-mutant (mutTNF) and shown that mutTNF efficiently inhibits TNFR1-mediated bioactivity *in vitro* and attenuates inflammatory conditions *in vivo*. In this study, we aimed to improve the TNFR1-selectivity of mutTNF. This was achieved by constructing a phage library displaying mutTNF-based variants, in which the amino acid residues at the predicted receptor binding sites were substituted to other amino acids. From this mutant TNF library, 20 candidate TNFR1-selective antagonists were isolated. Like mutTNF, all 20 candidates were found to have an inhibitory effect on TNFR1-mediated bioactivity. However, one of the mutants, N7, displayed significantly more than 40-fold greater TNFR1-selectivty than mutTNF. Therefore, N7 could be a promising anti-autoimmune agent that does not interfere with TNFR2-mediated signaling pathways.

1. Introduction

The severity and progression of inflammatory diseases, such as rheumatoid arthritis, Crohn's disease and ulcerative colitis, can be correlated with the serum level of tumor necrosis factor-α (TNF). Thus, TNF blockades such as anti-TNF antibodies and soluble TNFRs, which neutralize the activity of TNF, have been used to treat various autoimmune diseases in clinical practice. However, TNF blockades inhibit both TNFR1 and TNFR2 signaling. Thus, treatment with these drugs can lead to an increased risk of infection (Gomez-Reino et al. 2003; Lubel et al. 2007) and lymphoma development (Brown et al. 2002). TNF has been reported to induce inflammatory response predominantly through TNFR1 (Mori et al. 1996), whereas activation of the immune response is initiated *via* TNFR2 (Kim et al. 2006; Kim and Teh 2001; Grell et al. 1998). Therefore, blocking TNFR1-signaling, but not TNFR2-signaling, is a promising strategy for the safe and effective treatment of inflammatory diseases, which overcomes the risk of infection associated with the use of non-specific TNF blockades (Kollias and Kontoyiannis 2002).
In our previous studies, we used the phage display technique (Imai et al. 2008; Nagano et al. 2009; Nomura et al. 2007) to generate a TNFR1-selective antagonistic mutant TNF (mutTNF) that blocks TNFR1-mediated signals but not those of TNFR2 (Shibata et al. 2008b). Moreover, mutTNF showed superior therapeutic effects using an inflammatory disease mouse model (Shibata et al. 2008a). Thus, a drug for autoimmune diseases that selectively targets TNFR1 is anticipated to display higher efficacy and safety compared to existing treatments. In this study, we have attempted to isolate TNFR1-selective antagonists with higher TNFR1-selectivity than previous mutTNF by constructing a modified phage library displaying mutTNF-based variants.

2. Investigations, results and discussion

Here, we attempted to improve the TNFR1-selectivity of mutTNF using a phage display technique. Firstly, we constructed a phage library of TNF mutant using mutTNF as template. We designed a randomized library of mutTNF to replace the six amino acid residues (aa 29, 31, 32, 145–147) in the predicted receptor binding site. As a result of the 2-step PCR, we confirmed that the mutTNF mutant library consisted of 4×10^7 independent recombinant clones (*data not shown*). To enrich for TNFR1-selective antagonists, the phage library was subjected to two rounds of panning against TNFR1 on a Biacore biosensor chip. After the second panning, supernatants of single clone of *E. coli* TG1 including phagemid were randomly collected and subjected to screening by bioassay and ELISA to evaluate their bioactivity and affinity against each TNF receptor, respectively (*data not shown*). Consequently, twenty candidates of TNFR1-selective mutants with antagonistic activity were isolated (Table).
Next, we determined the detailed biological properties of each candidate. Positive clones were engineered for expression in

Table: Amino acid sequences and biological properties of TNFR1-selective antagonist candidates

TNF	Amino acid sequence						Relative affinity (% K_d)[a]			Bioactivity via TNFR1	
	29	31	32	145	146	147	TNFR1	TNFR2	TNFR1[b]/TNCR2	Agonistic[c] activity	Antagonisti[d] activity
mutTNF	L	R	R	A	E	S	100.0	100.0	1.0	–	+
N1	S	–	W	R	–	–	550.0	21.6	25.5	+	–
N2	S	–	W	–	–	–	200.0	N.D.	N.D.	+	–
N3	S	–	W	R	D	–	550.0	44.8	12.3	–	±
N4	S	–	W	–	D	–	183.3	19.1	9.6	±	–
N5	S	–	W	–	S	E	275.0	25.8	10.7	±	–
N6	A	D	T	–	–	–	200.0	21.6	9.3	±	–
N7	S	N	D	D	A	–	104.7	2.5	41.9	–	+
N8	R	I	A	D	–	–	169.2	26.7	6.3	+	–
N9	H	H	–	–	N	G	169.2	33.0	5.1	+	–
N10	T	N	N	–	–	–	314.3	28.6	11.0	±	–
N11	T	N	N	S	–	–	275.0	18.3	15.0	±	–
N12	F	S	T	–	–	–	440.0	58.0	7.6	+	–
N13	F	S	T	–	S	E	440.0	73.9	6.0	+	–
N14	R	W	Y	T	N	T	314.3	19.2	16.4	+	–
N15	F	K	T	N	A	T	275.0	24.1	11.4	±	–
N16	M	L	T	N	S	T	367.0	7.7	47.7	+	–
N17	Y	L	A	T	H	T	137.5	1.6	86.0	±	–
N18	Y	L	A	T	H	–	110.0	4.7	23.4	±	–
N19	V	Q	Y	N	N	–	367.0	N.D.	N.D.	±	–
N20	F	S	T	P	Q	R	244.4	N.D.	N.D.	±	–

Conserved residues compared with mutTNF are indicated by an em dash (–) The affinity values are shown as relative values (% mutTNF). N.D.: not detected

[a] Affinity for immobilized TNFR1 and TNFR2 was assessed by SPR using BIAcore3000. The dissociation constant (K_d) of TNF mutants were calculated from their sensorgrams by BIAEVALUATION 4.0 software

[b] TNFR1-selectivity was defined as relative affinity [TNFE1]/ relative affinity [TNFR2] for mutTNF

[c] TNFR1-mediated agonistic activity was measured, using a HEp-2 cell cytotoxicity assay. The intensity in agonistic activity was evaluated as the following. Cell viability at 10^4 ng/ml each mutant. 0–25% (of non treatment); (+), 25–50%; (±), 50–100%; (–)

[d] TNFR1-mediated antagonistic activity of mutant TNFs on wtTNF induced cytotoxicity in HEp-2 cells was measured. The intensity in antagonistic activity was evaluated as the following. Cell viability at 10^5 ng/ml each mutant in present of 5 ng/ml wtTNF. 0–25% (of non treatment); (–), 25–50%; (±), 50–100%; (+)

E. coli BL21λDE3 and each recombinant protein was purified as described previously (Yamamoto 2003). As anticipated, gel electrophoresis confirmed the mutant TNF proteins to have a molecular weight of 17 kDa. Moreover, gel filtration chromatography established that each mutant forms a homotrimeric complex in solution, as is the case for wild-type TNF (wtTNF) (*data not shown*). To analyze the binding properties of these TNFR1-selective TNF candidates, their dissociation constants (K_d) for TNFR1 and TNFR2 were measured using a surface plasmon resonance (SPR) analyzer. Our previous SPR analysis showed that although mutTNF has an almost identical affinity to TNFR1 as to wtTNF, it displays more than 17,000-fold greater selectivity for TNFR1. As shown in the Table, all the candidates exhibited higher affinity for TNFR1 than mutTNF. Furthermore, clones N1, N7, N16, N17 and N18 showed more than 20-fold higher TNFR1-binding selectivity compared to mutTNF. To examine the bioactivity of all candidates *via* TNFR1, we subsequently performed a cytotoxicity assay using

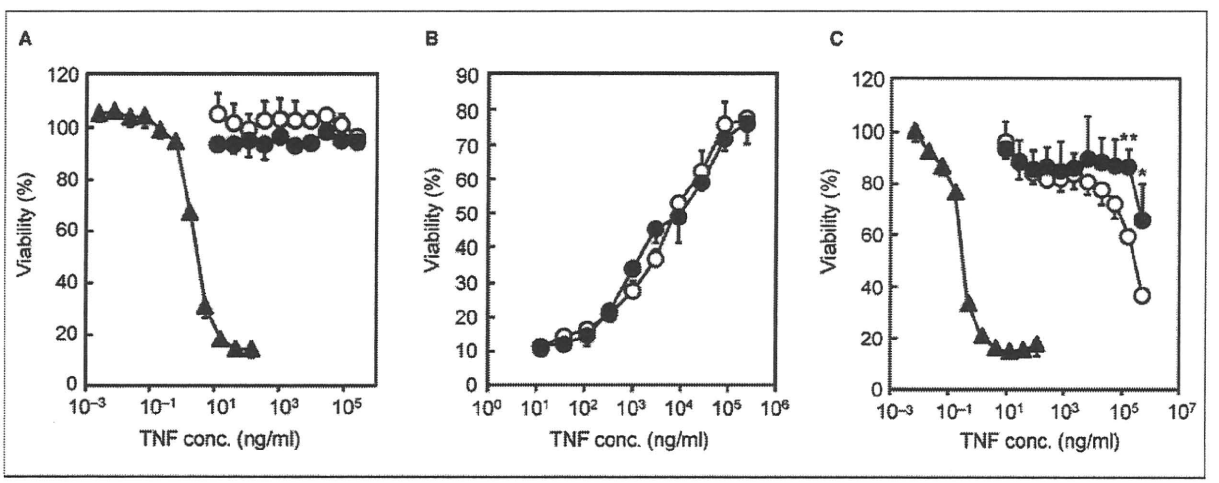

Fig.: Bioactivities and antagonistic activities of N7. (A) To determine the TNFR1-mediated bioactivities, several dilutions of wtTNF (closed triangle), mutTNF (open circle) and N7 (closed circle) were added to L-M cells and incubated for 4 h at 37 °C. (B) Indicated dilutions of mutTNF (open circle) and N7 (closed circle) and constant of wtTNF (5 ng/ml) were mixed and added to L-M cells and incubated for 4 h at 37 °C. TNFR1-mediated antagonistic activity was assessed as described in the Experimental section. (C) To determine the TNFR2-mediated bioactivities, diluted wtTNF (closed triangle), mutTNF (open circle) and N7 (closed circle) were added to hTNFR2/mFas-preadipocyte cells and incubated for 48 h at 37 °C. After incubation, cell viability was measured using the methylene blue assay. Data represent the mean ± S.D. and were analyzed by Student's t-test (*$p < 0,05$, **$p < 0,01$ vs mutTNF)

HEp-2 cells (Table). As anticipated, mutTNF was unable to activate TNFR1. Likewise clones N3 and N7 do not activate TNFR1 signaling, even when tested at high concentrations. The TNFR1-mediated antagonistic assay demonstrated that N7 showed the highest activity of all the TNFR1-selective antagonist candidates. The Figure show details of bioactivities and antagonistic activities of N7. The TNFR1-mediated agonistic activity using L-M cells showed that wtTNF displays TNFR1-mediated agonistic activity in a dose-dependent manner. In contrast, N7, in addition to mutTNF, barely displays any agonistic activity (Fig. A). Moreover, N7 had an almost identical antagonistic activity for TNFR1-mediated bioactivity to that of mutTNF (Fig. B). Next, TNFR2-mediated activities of these TNFR1-selective antagonists were measured using hTNFR2/mFas-preadipocyte cells. The bioactivity of mutTNF and N7 *via* TNFR2 was much lower than that of wtTNF. Remarkably, TNFR2-mediated agonistic activity of N7 was lower than that of mutTNF, in agreement with the reduced affinity for TNFR2 (Fig. C).

In conclusion, we have succeeded in creating a TNFR1-selective antagonist with improved TNFR1-selectivity over that of mutTNF. This was achieved by constructing a library of mutTNF variants using a phage display technique. While TNFR1 is believed to be important for immunological responses (Rothe et al. 1993), TNFR2 is thought to be important for antiviral resistance and is effective for controlling mycobacterial infection by affecting membrane-bound TNF stimulation (Saunders et al. 2005; Olleros et al. 2002). Therefore, use of N7 might reduce the risk of side effects, such as infections, when applying TNF blockade as a therapy for autoimmune disease. We are currently evaluating the therapeutic effect of N7 using a mouse autoimmune disease model.

3. Experimental

3.1. Cell culture

HEp-2 cells (a human fibroblast cell line) were provided by Cell Resource Center for Biomedical Research (Tohoku University, Sendai) and were maintained in RPMI 1640 medium supplemented with 10% FBS and 1% antibiotics cocktail (penicillin 10,000 units/ml, streptomycin 10 mg/ml, and amphotericin B 25 μg/ml). L-M cells (a mouse fibroblast cell line) were provided by Mochida Pharmaceutical Co. Ltd. (Tokyo, Japan) and were maintained in minimum Eagle's medium supplemented with 1% FBS and 1% antibiotics cocktail. hTNFR2/mFas-preadipocyte cells were established previously in our laboratory (Abe et al. 2008) and were maintained in Dulbecco's modified Eagle's medium supplemented with Blasticidin S HCl, 10% FBS, 1 mM sodium pyruvate, 5×10^{-5} M 2-mercaptoethanol, and 1% antibiotic cocktail.

3.2. Construction of a novel gene library displaying mutTNF variants

The pCANTAB phagemid vector encoding mutTNF was used as template for PCR. The mutTNF was created in previous study and showed TNFR1-selective antagonistic activity (Shibata et al. 2008b). The six amino acid residues at the receptor binding site (amino acid residues; 29, 31, 32 and 145–147) of mutTNF were replaced with other amino acids using a 2-step PCR procedure as described previously (Mukai et al. 2009).

3.3. Selection of TNFR1-selective antagonist candidates from a mutTNF mutated phage library

Human TNFR1 Fc chimera (R&D systems, Minneapolis, MN) was immobilized onto a CM3 sensor chip as described previously. Briefly, the phage display library (1×10^{11} CFU/100 μl) was injected over the sensor chip at a flow rate of 3 μl/min. After binding, the sensor chip was washed using the rinse command until the association phase was reached. Elution was carried out using 4 μl of 10 mM glycine-HCl. The eluted phage pool was neutralized with 1 M Tris-HCl (pH 6.9) and then used to infect *E. coli* TG1 in order to amplify the phage. The panning steps were repeated twice. Subsequently, single clones were isolated and supernatant from each clone was collected and used to determine the cytotoxicity in the HEp-2 cytotoxic assay and the affinity for TNFR1 by ELISA, respectively (Shibata et al. 2008b). We screened clones having almost no cytotoxicity but significant affinity for TNFR1. The phagemids purified from single clones were sequenced using the Big Dye Terminator v3.1 kit (Applied Biosystems, Foster City, CA). Sequencing reactions were analyzed on an ABI PRISM 3100 (Applied Biosystems).

3.4. Surface plasmon resonance assay (BIAcore® assay)

The binding kinetics of the proteins were analyzed by the surface plasmon resonance technique by BIAcore® (GE Healthcare, Amersham, UK). Each TNF receptor was immobilized onto a CM5 sensor chip, which resulted in an increase of 3,000–3,500 resonance units. During the association phase, all clones serially diluted in running buffer (HBS-EP) were allowed to pass over TNFR1 and TNFR2 at a flow rate of 20 μl/min. Kinetic parameters for each candidate were calculated from the respective sensorgram using BIAevaluation 4.0 software.

3.5. Cytotoxicity assay

In order to measure TNFR1-mediated cytotoxicity, HEp-2 or L-M cells were cultured in 96-well plates in the presence of TNF mutants and serially diluted wtTNF (Peprotech, Rocky Hill, NJ) with 100 μg/ml cycloheximide for 18 h at 4×10^4 cells/well or for 48 h at 1×104 cells/well. Cytotoxicity was then assessed using the methylene blue assay as described previously (Mukai et al. 2009; Shibata et al. 2004). For the TNFR1-mediated antagonistic assay, cells were cultured in the presence of 5 ng/ml human wtTNF and a serial dilution of the mutTNF. For the TNFR2-mediated cytotoxic assay, hTNFR2/mFas-preadipocyte cells were cultured in 96-well plates in the presence of TNF mutants and serially diluted wtTNF (1×10^4 cells/well) (Abe et al. 2008). After incubation for 48 h, cell survival was determined using the methylene blue assay.

Acknowledgement: This study was supported in part by Grants-in-Aid for Scientific Research from the Ministry of Education, Culture, Sports, Science and Technology of Japan, and by Grants-in-Aid for Scientific Research from Japan Society for the Promotion of Science (JSPS). In addition, this study was also supported in part by Health Labour Sciences Research Grants from the Ministry of Health, Labor and Welfare of Japan, Health Sciences Research Grants for Research on Publicly Essential Drugs and Medical Devices from the Japan Health Sciences Foundation and by a Grant from the Minister of the Environment, as well as THE NAGAI FOUNDATION TOKYO.

References

Abe Y, Yoshikawa T, Kamada H, Shibata H, Nomura T, Minowa K, Kayamuro H, Katayama K, Miyoshi H, Mukai Y, Yoshioka Y, Nakagawa S, Tsunoda S, Tsutsumi Y (2008) Simple and highly sensitive assay system for TNFR2-mediated soluble- and transmembrane-TNF activity. J Immunol Methods 335: 71–78.

Aggarwal BB (2003) Signalling pathways of the TNF superfamily: a double-edged sword. Nat Rev Immunol 3: 745–756.

Brown SL, Greene MH, Gershon SK, Edwards ET, Braun MM (2002) Tumor necrosis factor antagonist therapy and lymphoma development: twenty-six cases reported to the Food and Drug Administration. Arthritis Rheum 46: 3151–3158.

Feldmann M (2002) Development of anti-TNF therapy for rheumatoid arthritis. Nat Rev Immunol 2: 364–371.

Goldbach-Mansky R, Lipsky PE (2003) New concepts in the treatment of rheumatoid arthritis. Annu Rev Med 54: 197–216.

Gomez-Reino JJ, Carmona L, Valverde VR, Mola EM, Montero MD (2003) Treatment of rheumatoid arthritis with tumor necrosis factor inhibitors may predispose to significant increase in tuberculosis risk: a multicenter active-surveillance report. Arthritis Rheum 48: 2122–2127.

Grell M, Becke FM, Wajant H, Mannel DN, Scheurich P (1998) TNF receptor type 2 mediates thymocyte proliferation independently of TNF receptor type 1. Eur J Immunol 28: 257–263.

Imai S, Mukai Y, Takeda T, Abe Y, Nagano K, Kamada H, Nakagawa S, Tsunoda S, Tsutsumi Y (2008) Effect of protein properties on display efficiency using the M13 phage display system. Pharmazie 63: 760–764.

Kim EY, Priatel JJ, Teh SJ, Teh HS (2006) TNF receptor type 2 (p75) functions as a costimulator for antigen-driven T cell responses *in vivo*. J Immunol 176: 1026–1035.

Kim EY, Teh HS (2001) TNF type 2 receptor (p75) lowers the threshold of T cell activation. J Immunol 167: 6812–6820.

Kollias G, Kontoyiannis D (2002) Role of TNF/TNFR in autoimmunity: specific TNF receptor blockade may be advantageous to anti-TNF treatments. Cytokine Growth Factor Rev 13: 315–321.